

APPROVED FOR RELEASE: 2007/02/08: CIA-RDP82-00850R000200050040-0

21 FEBRUARY 1980 ELEC
EL
(FOUO 3/80)

1 OF 1

FOR OFFICIAL USE ONLY

JPRS L/8938

21 February 1980

USSR Report

ELECTRONICS AND ELECTRICAL ENGINEERING

(FOUO 3/80)



FOREIGN BROADCAST INFORMATION SERVICE

FOR OFFICIAL USE ONLY

NOTE

JPRS publications contain information primarily from foreign newspapers, periodicals and books, but also from news agency transmissions and broadcasts. Materials from foreign-language sources are translated, those from English-language sources are transcribed or reprinted, with the original phrasing and other characteristics retained.

Headlines, editorial reports, and material enclosed in brackets [] are supplied by JPRS. Processing indicators such as [Text] or [Excerpt] in the first line of each item, or following the last line of a brief, indicate how the original information was processed. Where no processing indicator is given, the information was summarized or extracted.

Unfamiliar names rendered phonetically or transliterated are enclosed in parentheses. Words or names preceded by a question mark and enclosed in parentheses were not clear in the original but have been supplied as appropriate in context. Other unattributed parenthetical notes within the body of an item originate with the source. Times within items are as given by source.

The contents of this publication in no way represent the policies, views or attitudes of the U.S. Government.

For further information on report content
call (703) 351-2938 (economic); 3468
(political, sociological, military); 2726
(life sciences); 2725 (physical sciences).

COPYRIGHT LAWS AND REGULATIONS GOVERNING OWNERSHIP OF
MATERIALS REPRODUCED HEREIN REQUIRE THAT DISSEMINATION
OF THIS PUBLICATION BE RESTRICTED FOR OFFICIAL USE ONLY.

FOR OFFICIAL USE ONLY

JPRS L/8938

21 February 1980

USSR REPORT
ELECTRONICS AND ELECTRICAL ENGINEERING
(FOUO 3/80)

This serial publication contains articles, abstracts of articles and news items from USSR scientific and technical journals on the specific subjects reflected in the table of contents.

Photoduplications of foreign-language sources may be obtained from the Photoduplication Service, Library of Congress, Washington, D. C. 20540. Requests should provide adequate identification both as to the source and the individual article(s) desired.

CONTENTS	PAGE
Communications; Communication Equipment; Data Transmission and Processing	1
Formation of Linear Frequency Modulated Signals and Processing of Them in an Acoustic Surface Wave Filter	1
Increasing the Effectiveness of the Reception of Signals in a Complex Noise Situation by Aggregate Repetition	5
Components and Circuit Elements, Including Filters and Band Lines	6
Approximate Calculation of Parameters of Band Filters Utilizing Acoustic Surface Waves	6
Experimental Investigation of Narrowband Matched Filters for Acoustic Surface Waves	15
Algorithm for Calculation of Shielded Band Lines	20
Electromagnetic Wave Propagation	29
Scattering of Modes of the Whispering Gallery Type by Ionospheric Inhomogeneities Along a Geomagnetic Field	29
Instruments, Measuring Devices and Testers; Methods of Measuring	42
Acousto-Optical Fourier Special Processor	42
Power Systems	46
Problems of Power Engineering at its Present Stage of Development	46

- a - [III - USSR - 21E S&T FOUO]

FOR OFFICIAL USE ONLY

FOR OFFICIAL USE ONLY

CONTENTS (Continued)	Page
Publications	55
Handbook on Acoustics	55
Handbook on Components of Microstrip Equipment	58
Signal Reception and Evaluation of Quality	61
Ultralong Range Propagation of Short Radio Waves	64
The Development of Research in Thermoelectricity in the USSR	66

- b -

FOR OFFICIAL USE ONLY

FOR OFFICIAL USE ONLY

Communications; Communication Equipment;
Data Transmission and Processing

UDC 621.376.32.621.396.662

FORMATION OF LINEAR FREQUENCY MODULATED SIGNALS AND PROCESSING OF THEM IN
AN ACOUSTIC SURFACE WAVE FILTER

Kiev IZVESTIYA VUZOV SSSR, RADIOELEKTRONIKA in Russian Vol 22 No 9, 1979
pp 73-75 manuscript received 3 Jul 78

[Article by L.A. Belov, S.S. Karinskiy and V.G. Komarov]

[Text] Modern requirements for accuracy in the formation of LChM [linear frequency modulated] signals are very high. For the purpose of producing at the output of the processing system a compressed signal with a side lobe level of -35 to -40 dB, the permissible deviations in the characteristics of the shaping and compression equipment in relation to phase are on the order of a few degrees, and in relation to amplitude on the order of a few percent [1].

For the purpose of satisfying these requirements, in active shapers it is necessary to employ systems for automatic tuning of the initial frequency and the rate of frequency modulation (AP LChM [2,3]), and the power level [4]. Modern processing units are based on the utilization of acoustic surface waves [5,6]. It is possible to rate the quality of shaping in relation to the instantaneous error signal of the AP LChM system's phase detector. Effective in addition is a rating in terms of the level of side lobes at the output of the combined shaping and compression system. This report is devoted to the development of such a system.

The structural diagram of an experimental mockup is shown in fig 1. A controlled oscillator, UG, employing a mitron, is encompassed by a ring for automatic phase tuning of the initial frequency, FAPCh, including a mixer, Sm2, filter, F2, and switch, K12. The initial frequency, f_0 , is a multiple of the frequency of the quartz oscillator, KG: $f_0 = n_1 f_k$. The reference delay line, LZ, with a time period of τ , mixer, Sm1, phase detector, FD, filter, F1, and switch, K11, form the AP LChM ring [2], by means of which the modulation rate, ω/T , is tuned to a value of $f_k/n_2\tau$, where ω and T are the frequency deviation and the length of the LChM signal and n_2 is the frequency division factor of the KG. Switch K12 is closed in the FAPCh mode, and switch K11 in the LChM mode, being repeated at a rate of f_k/n_2n_3 . The frequency division factor,

FOR OFFICIAL USE ONLY

Key :

- The acoustic surface wave (APV) compression filter is designed from a y-section quartz crystal acoustic line [5]. It contains one non-equi-distant opposing-pin-type transducer and another transducer with apodized electrodes, performing the role of a weighting filter with a cosine-type envelope and a pedestal of about 0.05. Both transducers are fabricated by the photolithographic method from silver 0.1 mm thick.

FOR OFFICIAL USE ONLY

The dispersing filter [6] was designed on the assumption that the number of pairs of electrodes in it would be restricted to $M \leq \sqrt{\omega T_s} / k_m^2$, where k_m is the electromechanical coupling coefficient, so that distortions as the result of diffraction and reflections are slight. Distance l_n from the first electrode to the n-th is found from the relationship $l_n = vt_n$, where v is the velocity of APV's and t_n represents the roots of the equation for the quadratic function of the phase, $f_n t_n + \omega t_n^2 / 2T_s = n/2$, where $n = 1, 2, 3, \dots$.

Measurements of an APV filter with an initial frequency f_n of about 20 MHz, a deviation of 7 MHz and a compression coefficient of n_{120} demonstrated that deviations in phase were not greater than 0.1 radians, and irregularity in relation to amplitude was less than three percent. When to the input of a dispersing filter with weighted processing was supplied the inverted response from a similar filter without weighted processing, compressed pulses were produced (fig 2) with a side lobe level close to the calculated, -35 to -40 dB.

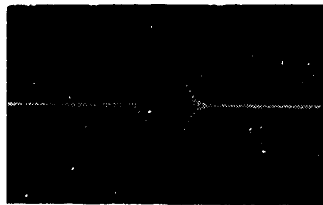


Figure 2.

Filters with weighted processing which utilize APV's were employed in a combined system for shaping and compressing an LChM signal according to the arrangement shown in fig 1. Investigations demonstrated good effectiveness in the operation of all three automatic tuning rings. Pickup of the UG's frequency with reference to the quartz standard took place in the initial frequency difference range of 7 to 8 MHz, and the transient process in the FAPCh system lasted no longer than 2 to 3 μs . Constancy of the LChM rate was monitored in terms of the change in phase of oscillations of the difference frequency in the output of the FD. It was shown that the LChM rate varies by not more than 0.1 percent. The compressed pulse at the output of Us2 is similar to that shown in fig 2, with a side lobe level of about -26 dB.

Thus, an investigation of a combined system for shaping and compressing an LChM signal has demonstrated good shaping quality and the high effectiveness of compression filters utilizing APV's with weighted processing.

FOR OFFICIAL USE ONLY

FOR OFFICIAL USE ONLY

Bibliography

1. Kuk, Ch. and Bernfel'd, M. "Radiolokatsionnyye signaly" [Radar Signals], Moscow, Sovetskoye Radio, 1971.
2. Belov, L.A. and Kochemasov, V.N. "Automatic Tuning of the Rate of Linear Frequency Modulation," RADIOTEKHNIKA, 1977, 32, No 8, pp 30-34.
3. Belov, L.A., Barabanov, V.B. and Kochemasov, V.N. "Discrete System for Automatic Tuning of the Frequency Modulation Principle," ELEKTRO-SVYAZ', 1973, No 5.
4. Kochemasov, V.N. and Belov, L.A. "Applications of LChM Signals and Methods of Shaping Them," ZARUBEZHNYAYA RADIOELEKTRONIKA, 1975, No 8.
5. Rechitskiy, V.I. and Singur, Ye.K. "Signal Generators Utilizing PAV's," ZARUBEZHNYAYA RADIOELEKTRONIKA, 1978, No 3, pp 95-108.
6. Karinskiy, S.S. "Ustroystva obrabotki signalov na ul'trazvukovykh poverkhnostnykh volnakh" [Signal Processing Equipment Utilizing Ultrasonic Surface Waves], Moscow, Sovetskoye Radio, 1975.

COPYRIGHT: IZVESTIYA VUZOV SSSR, RADIOELEKTRONIKA, 1979
[53-8831]

CSO: 1860
8831

FOR OFFICIAL USE ONLY

FOR OFFICIAL USE ONLY

USSR

UDC 621.396.62.391.8:621.512.54

INCREASING THE EFFECTIVENESS OF THE RECEPTION OF SIGNALS IN A COMPLEX NOISE
SITUATION BY AGGREGATE REPETITION

ELEKTROPROM-ST I PRIBOROSTROYENE in Bulgarian Vol 13 No 5, 1978 pp 208-210

RANGELOV, KAMEN V1.

[From REFERATIVNYY ZHURNAL RADIOTEKHNIKA No 1, 1979 Abstract No 1D1 from
the Resume]

[Text] The possibility is demonstrated of increasing the effectiveness of
reception of signals by aggregate repetition and by the use of the structur-
al properties of signals and noise. A quantitative criteria is developed
and used for evaluation of the effectiveness of reception.
[-6508]

FOR OFFICIAL USE ONLY

FOR OFFICIAL USE ONLY

Components and Circuit Elements, Including
Filters and Band Lines

UDC 534.86

APPROXIMATE CALCULATION OF PARAMETERS OF BAND FILTERS UTILIZING ACOUSTIC
SURFACE WAVES

Kiev IZVESTIYA VUZOV SSSR, RADIOELEKTRONIKA in Russian Vol 22 No 9, 1979
pp 56-60 manuscript received 28 Jun 78, after revision 14 Nov 78

[Article by V.A. Videnko, I.M. Grankin, Ye.A. Nelin and V.P. Pogrebnyak]

[Text] Approximate equations are obtained for calculating the parameters of band filters utilizing acoustic surface waves (PAV's). On the basis of a comparison of the values of parameters calculated by the approximate equations and by a precise model for analyzing filters utilizing PAV's, it is demonstrated that the error of the approximate equations is totally acceptable in engineering calculations.

The familiar methods of synthesizing and analyzing filters utilizing acoustic surface waves (PAV's) have made it possible to develop filters satisfying high technical requirements [1]. But these methods are complex and require considerable expenditures of computer resources.

Approximate equations are required for a quick estimate of the parameters of band filters utilizing PAV's in an engineering calculation. These equations can be arrived at on the basis of a model of equivalent circuits of a filter utilizing PAV's [2] with some simplifications. We will discuss a filter formed by apodized and non-apodized transducers, since this design is used most frequently. The results arrived at can be utilized also for calculating other designs. The simplifications are based firstly on replacing with a sinc x function the apodization function of an apodized transducer synthesized by different methods and, secondly, by taking into account only the main and first side lobes of the sinc x function. We will indicate the justification for this approach.

The apodization function is equal to an inverse Fourier transform of the required amplitude-frequency characteristic (AChKh) placed at the origin. The sinc x apodization function is characteristic of a rectangular band AChKh. Here $x = \Delta f t$, where Δf is the width of the passband. Of course, a rectangular AChKh is physically unrealizable. In this case this is associated with the fact that the dimensions of the transducer are finite.

FOR OFFICIAL USE ONLY

FOR OFFICIAL USE ONLY

For the purpose of realizing a band AChKh approximating a rectangular one, in the simplest method of synthesis function $\text{sinc } x$ must be weighted in keeping with the law of one of the weighting functions in [3]. If function $\text{sinc } x$ is multiplied by a rectangular weighting function, then the AChKh in this case will be most rectangular, but the levels of non-uniformity in the passband and side lobes produced then are unacceptable for the majority of applications. A function weighted in keeping with any other law will differ from function $\text{sinc } x$ to a greater extent, the worse the rectangularity of the AChKh. In weighting, reduced to the greatest extent are the values of function $\text{sinc } x$ in long-range lobes, and to the least, values in the main lobe. It is obvious that in synthesizing an apodized transducer by other methods the apodization function will differ from function $\text{sinc } x$ in keeping with the same rules. The maximum value of function $\text{sinc } x$ in the first side lobe equals 0.2, and in the second, 0.13. With a weighted function these values are even lower. Therefore we will take into account only the main and first side lobe of function $\text{sinc } x$.

The parameters of an apodized transducer are calculated in the following manner [2]. An apodized transducer is conventionally divided by horizontal lines into bands of identical width. The bands represent non-apodized transducers. The parameters of a non-apodized transducer are easily calculated by the familiar equations. The parameters of an apodized transducer are found by summing the parameters of bands.

The static capacitance of a non-apodized transducer [2] equals

$$C_0 = WC_s/2(N-1), \quad (1)$$

where W is the converter's aperture; $C_s/2$ is the capacitance of two electrodes per unit of their overlap; and N is the number of electrodes. The static capacitance of an apodized transducer equals

$$C_0 = \sum_{i=1}^m C_s/2 (N_i - 1) \Delta W,$$

where m is the number of bands; N_i is the number of electrodes in the i -th band; ΔW is the bandwidth. The accuracy of the calculation increases with a reduction in ΔW . Product $(N_i - 1)\Delta W$ represents the sum of the amount of overlap of electrodes in the band.

$$\sum_{i=1}^m (N_i - 1) \Delta W$$

is the sum of overlaps of electrodes of m bands. If ΔW approaches zero, then

$$\sum_{i=1}^m (N_i - 1) \Delta W$$

FOR OFFICIAL USE ONLY

FOR OFFICIAL USE ONLY

will approach the sum of overlaps of the converter's electrodes,

$$\sum_{n=1}^{2N-1} W_n,$$

where $2N$ is the number of electrodes and W_n is the size of the n -th overlap of electrodes. Taking into account the symmetry of the structure of an apodized transducer with regard to the central electrode overlap,

$$C_0 = C_s \left(W/2 + \sum_{n=2}^N W_n \right). \quad (2)$$

Let us consider the area beneath the apodization function curve, $W(t)$:

$$S = \int_0^{\tau/2} W(t) dt,$$

where τ is the length of the transducer's pulse characteristic. Function $W(t)$ varies insignificantly between the axes of symmetry of neighboring electrodes, i.e., within a range of variation of t by an amount of $1/(2f_0)$, where f_0 is the central frequency. Let us assume that function $W(t)$ does not vary within these limits. In this case $W(t)$ will be a step function:

$$W(t) = W, \quad 0 \leq t < \frac{1}{4f_0},$$

$$W(t) = W_n, \quad \frac{2n-3}{4f_0} \leq t < \frac{2n-1}{4f_0}, \quad n = 2, \dots, N.$$

Then

$$S \approx 2 \left[W \int_0^{1/4f_0} dt + W_2 \int_{1/4f_0}^{3/4f_0} dt + \dots + W_N \int_{(2N-3)/4f_0}^{(2N-1)/4f_0} dt \right] = \frac{1}{f_c} \left(\frac{W}{2} + \sum_{n=2}^N W_n \right).$$

Comparing this expression with (2), we get

$$C_0 \approx C_s f_0 = 2C_s f_0 \int_0^{\tau/2} W(t) dt.$$

FOR OFFICIAL USE ONLY

Let us substitute as the apodization function the function $W \operatorname{sinc} \Delta f t$, limited to the two lobes,

$$C_0 \approx \frac{2C_s W f_0}{\pi \Delta f} \int_0^{2\pi} \left| \frac{\sin \pi \Delta f t}{\pi \Delta f t} \right| d(\pi \Delta f t).$$

We find the value of

$$\int_0^{2\pi} \left| \frac{\sin x}{x} \right| dx$$

by employing the function

$$\operatorname{Si}(x) = \int_0^x \frac{\sin x}{x} dx,$$

the values of which have been tabulated,

$$\int_0^{2\pi} \left| \frac{\sin x}{x} \right| dx = \operatorname{Si}(\pi) + (\operatorname{Si}(\pi) - \operatorname{Si}(2\pi)) = 2.3.$$

Thus,

$$C_0 \approx 1.5 C_s W f_0 / \Delta f. \quad (3)$$

Since Δf is the width of the passband of a rectangular band AChKh, then as Δf it is necessary to substitute a value equal to the sum of the width of the passband and the width of the transition band of the AChKh of an apodized transducer. For an AChKh with high rectangularity, the width of the passband is severalfold greater than the width of the transmission band; therefore it is possible to disregard the latter in this case.

The active component of the input admittance of a non-apodized transducer at the central frequency [2] is $G_a = 2k^2 C f_0 W N^2$, where k is the electromechanical coupling factor. The active component of the input admittance of an apodized transducer, taking into account its symmetry with regard to the central overlap of electrodes and the horizontal line connecting the middle of the overlaps, is $G_a = 16k^2 C f_0 \sum_{i=1}^N N^2 \Delta W$. If $\Delta W \rightarrow 0$, then $\sum_{i=1}^N N^2 \Delta W$ will approach $\int_0^1 N^2(y) dy$. In calculating G_a we will take into account only the main lobe of function $\operatorname{sinc} x$. We determine $N^2(y)$ from the equation

FOR OFFICIAL USE ONLY

$$y = \frac{1}{2} \frac{\sin \pi \Delta f / 2 f_0 N(y)}{\pi \Delta f / 2 f_0 N(y)}.$$

Let us designate $\pi \Delta f / 2 f_0 = M$. Let us employ the expansion of function $\sin x$ into a series and limit ourselves to three of its terms,

$$\sin x \approx \frac{x}{1!} - \frac{x^3}{3!} + \frac{x^5}{5!}, \text{ i.e. } \frac{\sin x}{x} \approx 1 - \frac{x^2}{6} + \frac{x^4}{120}.$$

Substituting $x = MN(y)$, we get

$$N^4(y) - 20/M^2 N^2(y) + 120/M^2 (1 - 2y) = 0.$$

The solution to this equation is

$$N^2(y) = \frac{10 - 2\sqrt{5}\sqrt{12y - 1}}{M^2}.$$

Taking into account that permissible values of $y \geq 1/12$, we get

$$\int_0^{1/2} N^2(y) dy \approx \int_{1/12}^{1/2} \frac{10 - 2\sqrt{5}\sqrt{12y - 1}}{M^2} dy = \frac{25}{18M^2}.$$

(4)

Thus,

$$G_s \approx 9k^2 C f_0 W (f_0 / \Delta f)^2.$$

In figs 1a and 1b are given calculated dependences of the static capacitance and active component of admittance of an apodized transducer synthesized by the iteration optimization method in [3], on the relative width of the passband of its AChKh. Curves are plotted from equations (3) and (4) and by the dots are indicated the upper and lower limits of variations in values of parameters arrived at from the equivalent circuit model in [2], with a change in number of electrodes from 60 to 200. The width of the transmission band equals two percent, the level of irregularity in the passband 0.5 dB, the aperture is 5 mm and the central frequency is 30 MHz. Obviously, the approximate equations produce an error totally acceptable for engineering calculations.

FOR OFFICIAL USE ONLY

FOR OFFICIAL USE ONLY

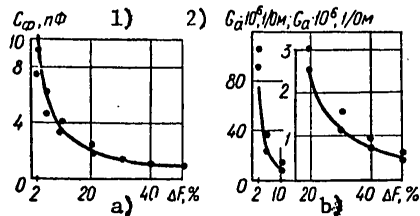


Figure 1.

Key:

1. pF

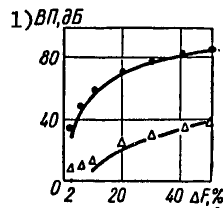
2. $G_a \cdot 10^6, 1/\Omega$ 

Figure 2.

Key:

1. Induced losses, dB

Let us note that the equations for calculating C_0 and G_a of a non-apodized transducer differ from the respective equations for an apodized, by the fact that in place of magnitude N in these equations is included magnitude $2f_0/\Delta f$, and the constant factors differ slightly. (In (1) difference $N-1 \approx N$, since $N \gg 1$). Usually the number of electrodes of a non-apodized transducer is determined on the basis of the condition that the passband of its AChKh for the 3 dB level will equal that required for the filter, $\Delta f'$: $N = 1.77f_0/\Delta f'$. With high rectangularity of the AChKh, $N = 1.77f_0/\Delta f$, i.e., the values of parameters for an apodized and non-apodized transducer differ insignificantly.

According to [2] the value of the voltage transmission coefficient of a filter at the central frequency can be found from the equation

FOR OFFICIAL USE ONLY

FOR OFFICIAL USE ONLY

$$K = \left| \frac{(G_s + G_0 + j\omega_0 C_0)(G'_s + G_u + j\omega_0 C'_0) - Y_{21}^2}{-Y_{21}G_0} \right|, \quad (5)$$

where G_0 is the intrinsic conductance of the oscillator; G_u is the conductance of the load; Y_{21} is the direct transfer admittance at the central frequency; and the primes indicate the parameters of a non-apodized transducer.

It is easy to demonstrate that

$$G_{21} = |Y_{21}| = 4k^2 C_s f_0 N' \left(\frac{W}{2} + \sum_{n=2}^N (-1)^{L+1} W_n \right),$$

where L is the number of the lobe of the apodization function. Reasoning similarly as in calculating C_0 , it is possible to demonstrate that

$$\frac{W}{2} + \sum_{n=2}^N (-1)^{L+1} W_n \approx 2 \int_0^{T/2} W(t) dt.$$

Substituting under the integral sign function $W \sin \Delta f t$, limited to two lobes, we get

$$G_{21} \approx 4k^2 C_s f_0 W N' 2f_0 / \pi \Delta f \int_0^{2\pi} \sin \Delta f t d(\pi \Delta f t) = 3,6k^2 C_s f_0 W N' f_0 / \Delta f.$$

If $N' \approx 1.77f_0 / \Delta f$, then $G_{21} = 0.7G_a$.

Usually fulfilled are the conditions

$$G_0 \gg G_s, \quad G_0 \gg \omega_0 C_0, \quad G_u \gg G'_s, \quad G_u \gg \omega_0 C'_0 \quad (6)$$

(a severalfold excess is required). Taking this equation into account, (5) can be simplified, $K \approx G_u / G_{21}$. According to [2] the value of induced losses of the filter at the central frequency equals

FOR OFFICIAL USE ONLY

FOR OFFICIAL USE ONLY

$$B\pi = 10 \lg \frac{G_0}{4G_n} K^2, \text{ i.e., } B\pi \approx -20 \lg \frac{2G_{21}}{\sqrt{G_0 G_n}}.$$

If $G_0 = G_n$ and $N' \simeq 1.77 f_0 / \Delta f$, then, substituting the value of G_{21} , we get

$$B\pi \approx -20 \lg 12, 7 R_0 k^2 C_s f_0 W \left(\frac{f_0}{\Delta f} \right)^2, \quad (7)$$

where $R_0 = 1/G_0$.

In fig 2 are shown calculated dependences of induced losses of filters with apodized transducers, the dependences of whose parameters are shown in figs 1a and 1b. The internal resistance of the oscillator and the load resistance equal 75Ω . The curves correspond to (7) and the dots and triangles indicate the values of induced losses arrived at from the model of equivalent circuits for the quartz of the ST section and the lithium niobate of the YZ section, respectively. In changing the number of electrodes from 60 to 200, the values of induced losses change over the range of 1 to 2 dB. The conditions in (6) are fulfilled for quartz over the entire range of variation of the relative width of the passband, and for lithium niobate only starting with 10 percent.

In conclusion, let us mention two important conclusions which result from an analysis of equation (7). When the relative width of the passband is increased δ -fold, the induced losses (VP's) are increased by $40 \log \delta$ dB. The difference between induced losses for a filter fabricated with substrates made out of different materials is

$$\Delta B\pi = -20 \lg \frac{k^2 C_s}{k_1^2 C_{s1}}.$$

Substituting in this equation the parameters of the quartz of the ST section and the lithium niobate of the YZ section, we get $\Delta VP = 47$ dB.

Bibliography

1. Kheys and Khartmann. "Equipment Utilizing Surface Acoustic Waves for Communications Equipment," TITER, 1976, 64, No 5, p 98.
2. Matthaei, C.L. et al. "Simplifications for the Analysis of Interdigital Surface-Wave Devices," IEEE TRANS., 1975, SU-22, N 2, p 105.

FOR OFFICIAL USE ONLY

FOR OFFICIAL USE ONLY

3. Rabiner, L. and Gold, B. "Teoriya i primeneniye tsifrovoy obrabotki signalov" [Theory and Application of Digital Processing of Signals], Moscow, Mir, 1978.

COPYRIGHT: IZVESTIYA VUZOV SSSR, RADIOELEKTRONIKA, 1979
[53-8831]

CSO: 1860
8831

FOR OFFICIAL USE ONLY

FOR OFFICIAL USE ONLY

UDC 621.396.966

EXPERIMENTAL INVESTIGATION OF NARROWBAND MATCHED FILTERS FOR ACOUSTIC SURFACE WAVES

Kiev IZVESTIYA VUZOV SSSR, RADIOELEKTRONIKA in Russian Vol 22 No 9, 1979
pp 71-73 manuscript received 22 Mar 78, after revision 27 Dec 78

[Article by A.Ye. Znamenskiy and Ye.S. Muratov]

[Text] The transmission function (PF) of an opposing-pin-type transducer (VShP) with a constant aperture governing the PF of a filter matched with a square radio pulse (SF) is [1]:

$$H(\omega) = H_0 \{ \sin [(\omega_0 - \omega) \tau / 2] / [(\omega_0 - \omega) \tau / 2] \} \exp (i\omega\tau/2), \quad (1)$$

where H_0 is a constant factor; ω_0 and ω are the mean and instantaneous angular frequency, respectively, $\tau = 1/R$ is the length of the radio pulse; and R is the rate of transmission of binary information.

Let us transform expression (1) into the form

$$H(\omega) \cong H_{01} \{ \sin [(\omega_0 - \omega) \tau / 2^{N+1}] / [(\omega_0 - \omega) \tau / 2^{N+1}] \} \times \\ \times \exp (i\omega\tau/2^{N+1}) \prod_{h=1}^N [1 + \exp (i\omega\tau/2^h)], \quad (2)$$

where H_{01} is a constant factor and $N = 1, 2, 3, \dots$ is a whole number. The approximation sign in equation (2) is associated with the discrete structure of a VShP, in which can be contained only a whole number of pins spaced from one another in relation to the delay by a value of $1/2f_0$. But an analysis of equation (2) shows that the accuracy of the approximation is sufficiently high (not worse than 0.03 R) for the low transmission rate of $R \leq 300$ kbauds and intermediate frequencies in the 10 to 100 MHz band, discussed in this article, with low values of N , which completely satisfies the requirements for the parameters of an SF [2].

FOR OFFICIAL USE ONLY

FOR OFFICIAL USE ONLY

It follows from equation (2) that it is possible to synthesize required function $H(\omega)$ by means of a cascade connection of the SF for a transmission rate of $2^N R$ and a bank of N comb filters (GF's). Examples of this type of implementation for a filter for acoustic surface waves (PAV's) for $N = 1$ and $N = 2$ are given in figs 1a and 1b, respectively. Here two-section VShP's form an amplitude-frequency characteristic (AChKh) of the comb type, and non-angled equidistant VShP's, an AChKh of an SF for a transmission rate of $2^N B$. The letter M in fig 1 designates the metalized coating between sections of the GF. Let us note that the method of implementation shown in fig 1b makes it possible to shorten almost two-fold the lengthwise dimensions of the acoustic line, as compared with the method of implementation in fig 1a, which is especially important for low information transmission rates of $R = 5$ to 25 kbauds. A distinctive feature of narrowband PAV filters is the need to fine tune the mid-band frequency, f_0 , deviations of which from the calculated value are caused chiefly by the discrepancy in the speed of PAV's from one model of an acoustic line to another (on the order of $\pm 3 \cdot 10^{-2}$ percent for synthetic quartz), and by the deviation in the rate of propagation of PAV's in metalized sections of the VShP as the result of a technologically related discrepancy in parameters of the metalized structure [3]:

$$(V - V_m)/V = \gamma h \omega / V, \quad (3)$$

where V and V_m are the velocities of PAV's on the free and metalized surfaces, respectively; h is the thickness of the metalization; and γ is a factor depending on the materials of the metalization and acoustic line.

Fine tuning in relation to frequency Δf_0 can be performed, e.g., by partial removal of the metalization, M , between sections of the GF (fig 1):

$$\Delta f_0 = (\Delta V_s / V) f_0, \quad (4)$$

where ΔV is the equivalent change in the velocity of PAV's between sections of the GF on account of removal of a section of metalization;

$$V = V_m - (k^2/2) V, \quad (5)$$

where k is the electromechanical coupling coefficient of the material of the acoustic line.

By increasing the number of degrees of expansion of N in equation (2), it is possible to improve the accuracy of realization of the transmission function of a matched filter (SF) in tuning to f_0 . Physically this means that the band of the middle lobe of the AChKh is expanded in the

FOR OFFICIAL USE ONLY

FOR OFFICIAL USE ONLY

case of a high-speed SF inside of which the combs of the entire bank of GF's are tuned simultaneously. Calculations have demonstrated that for the two-element structure ($N = 2$) in fig 1b, in particular, it is possible to tune the mid-band frequency of f_0 within the range of 8 ± 40 percent of R while satisfying certain requirements for the parameters of an SF [2].

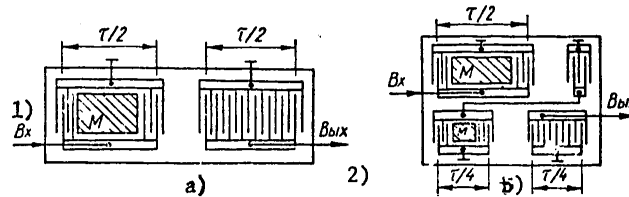


Figure 1.

Key:

1. In

2. Out

Let us give the results of the development of an SF for an OFT [relative phase telegraphy] demodulator for an information transmission rate of $R = 272$ kbauds and with $f_0 = 70 + 0.006$ MHz with a required accuracy in realization of the passband of $F = 0.885R = 240$ kHz, of not worse than ± 10 kHz, and with a deviation in the level of the first side lobe from the calculated of not greater than ± 2 dB. Since the possible frequency variance resulting from deviation in velocity in the quartz wafers is $\pm 3 \cdot 10 f_0 = \pm 21$ KHz, or less than 10 percent of R , then the decision was made to construct an SF with a single-element structure according to the type in fig 1a. As the material for the acoustic line was chosen an ST-section quartz wafer; the dimensions of the acoustic line were $32 \times 10 \times 2$ mm; and the metalized coating was chemically deposited silver with a thickness of $t = 0.08 \mu$.

For the purpose of measuring the mid-band frequencies of the two transducers (a GF and SF with a 2F band), in the center of the wafer was placed a broadband measuring VShP. The measured values of the mid-band frequencies equaled $f_0 = 70.014$ MHz for the SF and $f_0 = 69.990$ MHz for the GF. The amount of metal which it was necessary to clean away, ΔL , was determined on the basis of equations (3) to (5), where $\gamma = 0.52$ and $k^2 = 0.0012$; the calculated value of $\Delta L = 130 \mu$, corresponding to a tuning slope of $13 \mu/\text{kHz}$.

Cleaning away the metal with a diamond cutter by means of a UIM-21 microscope, with a precision of $\pm 3 \mu$, which corresponds to a method precision of not worse than 0.25 kHz at this frequency, resulted in a mid-band frequency for the GF of 70.001 MHz. The discrepancy from the calculated value

FOR OFFICIAL USE ONLY

FOR OFFICIAL USE ONLY

is related to the approximate nature of the equations used, (3) to (5), and to measurement errors. The resulting AChKh of the SF has a deviation in the level of the first side lobes from the theoretical in the range of ± 1.5 dB; the passband for the -3 dB level equaled 232 kHz. The experimental results, thus, agree sufficiently well with the calculated. For comparison let us note that the method of fine tuning f_0 discussed in [2], by etching away the VShP's metalization depthwise, taking into account technological errors in its implementation, is less accurate than the method discussed here by an order of magnitude (the accuracy of etching away the metal film is 10 to 20 percent of the thickness of the coating). In [4] the fine tuning of f_0 is accomplished by spraying a dielectric film onto the VShP. An evaluation of the accuracy of this method, made by means of graphs obtained, shows that it is less accurate than the one discussed here by one to two orders of magnitude.

Another method of electrically fine tuning the mid-band frequency is implemented by the connection of a phase inverter at an angle of ϕ between sections sections of the GF. The tuning then equals:

$$\Delta f_0 = (\varphi/2\pi n) f_0. \quad (6)$$

where n is the number of wavelengths, $\lambda = V/f_0$, confined between the centers of sections of the GF.

For the purpose of testing electrical frequency tuning, an SF was used for $f_0 = 12.003$ MHz and $R = 25.6$ kbauds, synthesized according to the arrangement in fig 1b by the cascade connection of two elements in an acoustic line consisting of an ST section of quartz measuring $100 \times 20 \times 5$ mm. After measurement of the mid-band frequencies in each element of the SF, they turned out to equal $f_0 = 12.003$ MHz.

Since the GF of the upper element basically determines the AChKh of the SF, then we will tune the mid-band frequency of precisely this GF. In each section of the GF of the upper element are contained 25 pairs of electrodes; the distance between the centers of GF sections equals 62 mm; the capacitance of the sections is $C = 10$ pF with an aperture of 4 mm; and the spacing of electrodes is every 0.131 mm (between centers). The phase shift in the current passing through separate sections of the GF's transducer was made possible in the experiment by installing in one section a series active variable resistance, r_p . A series variable capacitor, C_p , in another section served the purpose of equalizing the amplitudes of signals transmitted by sections in the introduction of the phase shift,

$$\varphi \approx (\arctg(r_p/2\pi/C)), \quad (7)$$

where C is the static capacitance of the transducer.

FOR OFFICIAL USE ONLY

Not taken into account in equation (7) is the series effective radiation resistance. Taking into account the fact that the Q of sections of the GF transducer is sufficiently high, this value can be disregarded.

In an experiment, in changing r from zero to $r = 1/(2\pi f_0 C)$, which corresponds to $\phi = \pi/4$, tuning^p of the mid-band frequency of the GF's effective peak was achieved at $f_0 = 6$ kHz or 0.13 kHz/degree, which has been confirmed by calculation according to equation (6). The deviation in the shape of the SF's AChKh thereby, within the frequency difference range of $\pm 2R$, does not exceed the limits of the requirements for parameters of an SF [2]. An evaluation with equations (6) and (7) demonstrates that replacing in the tuned SF the controllable resistor and capacitor with fixed ones with a precision of ± 5 percent and with temperature coefficients on the order of 10^{-3} /degree makes it possible to achieve tuning accuracy of not worse than 0.6 kHz in the temperature range of $\pm 50^\circ\text{C}$ with a maximum frequency difference of $\Delta f_0 < 6$ kHz. The precision of the method is improved considerably by increasing the accuracy of the rating of the resistor installed in the phase inverter and by lowering its TKR.

In experiments conducted with more complicated 0 to 180° phase inverters, tuning of $\Delta f_0 = 18$ kHz was achieved for the same speed of $R = 25$ kbauds. Therefore, with such low transmission rates, R , the electrical method of fine tuning is feasible to use for relatively not too high intermediate frequencies of $f_0 \leq 50$ MHz, at which the difference in speeds in acoustic lines does not exceed the limits of the tuning range.

Thus, both methods described here of fine tuning the mid-band frequency of an SF are simple and practical and ensure high accuracy, which has been confirmed by experiments.

Bibliography

1. Hartmann, C.S. "Impulse Model Design of Acoustic Surface Wave Filters," IEEE TRANS., 1973, MTT-21, N 4, p 162-175.
2. Hayld, W.H. "Precision Narrowband Surface Wave Bandpass Filters" in "IEEE Ultrasonics Symposium, Proc., 1974," pp 429-432.
3. Karinskiy, S.S. "Ustroystva obrabotki signalov na ul'trazvukovykh poverkhnostnykh volnakh" [Signal Processing Equipment Utilizing Ultrasonic Surface Waves], Moscow, Sovetskoye Radio, 1975.
4. Nishikawa, K. "An Improved Surface Acoustic Wave Filter for a PCM Timing Tank" in "IEEE Ultrasonics Symposium, Proc., 1974," pp 164-167.

COPYRIGHT: IZVESTIYA VUZOV SSSR, RADIOELEKTRONIKA, 1979
[53-8831]

CSO: 1860
8831

FOR OFFICIAL USE ONLY

UDC 621.372.04.75

ALGORITHM FOR CALCULATION OF SHIELDED BAND LINES

Kiev IZVESTIYA VUZOV SSSR, RADIOELEKTRONIKA in Russian Vol 22 No 9, 1979
pp 23-28 manuscript received 30 Jun 78, after revision 4 Dec 78

[Article by S.N. Arzhanov, S.A. Markova, S.B. Rayevskiy and V.Ya. Smorgonskiy]

[Text] An algorithm is suggested for calculating in a quasi-static approximation the unit-length parameters of shielded band lines. The results are given of a numerical investigation of the algorithm suggested, and estimates are also made of its accuracy and of the agreement of the solutions arrived at.

The wide employment in practice of shielded band and microband lines has made topical the problem of creating general (basic) algorithms for calculating their key characteristics, distinguished by universality, simplicity of the structural layout, good speed of response and high accuracy. In this study is discussed a rectangular shielded band line, shown in fig 1a, which can be regarded as the basic model for the calculation of more complex band lines. Mention should be made of the fact that a particular variant of it--a rectangular coaxial line--has also found independent application in attenuators, frequency multipliers, and in microwave gas spectroscopy--as absorbing Stark elements, in different oscillatory systems employing solid-state electronic devices and the like.

Let us divide each quadrant of the cross section of a microband line (fig 1a) into three regions, I, II and III. The general solution to the Laplace equation (the calculation is made in a quasi-T-wave approximation) satisfying the condition $E_{\tau}/S_{1,2} = 0$ ($S_{1,2}$ represents the surfaces of the line's conductors) we write in the form:

$$\bar{\Pi}_{zi} = \left\{ U_0 \frac{b_2 - y}{d_2} + \sum_{m=1}^{\infty} \left(A_m \operatorname{ch} \frac{\pi m}{d_2} x + A_m^* \operatorname{sh} \frac{\pi m}{d_2} x \right) \times \right. \\ \left. \times \sin \frac{\pi m}{d_2} (b_2 - y) \right\} e^{-i\omega \sqrt{\epsilon_3 \mu_3} z},$$

FOR OFFICIAL USE ONLY

FOR OFFICIAL USE ONLY

$$\Pi_{z2}^e = \left\{ U_0 \frac{b_2 - y}{d_2} \frac{a_2 - x}{d_1} + \sum_{m=1}^{\infty} C_m \sin \frac{\pi m}{d_2} (b_2 - y) \operatorname{sh} \frac{\pi m}{d_2} (a_2 - x) + \right. \\ \left. + \sum_{n=1}^{\infty} D_n \sin \frac{\pi n}{d_1} (a_2 - x) \operatorname{sh} \frac{\pi n}{d_1} (b_2 - y) \right\} e^{-i\omega \sqrt{\epsilon_3} \mu z};$$

$$\Pi_{z3}^e = \left\{ U_0 \frac{a_2 - x}{d_1} + \sum_{n=1}^{\infty} \left(B_n \operatorname{ch} \frac{\pi n}{d_1} y + B_n^* \operatorname{sh} \frac{\pi n}{d_1} y \right) \times \right. \\ \left. \times \sin \frac{\pi n}{d_1} (a_2 - x) \right\} e^{-i\omega \sqrt{\epsilon_3} \mu z},$$

where Π_1^e , Π_2^e and Π_3^e are electrical Hertz vectors in regions I, II and III (fig 1a), respectively; $d_1 = a_2 - a_1$; $d_2 = b_2 - b_1$; and ϵ_e is the effective value of the dielectric constant in the line.

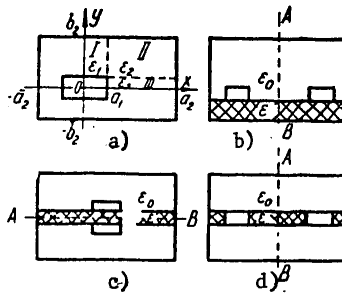


Figure 1.

From boundary conditions with $x = a_1$ and $y = b_1$, utilizing the property of orthogonality of eigenfunctions of regions I and III in intervals of $y \in [b_2, b_1]$ and $x \in [a_2, a_1]$, we get a system of linear algebraic equations in terms of amplitude factors:

FOR OFFICIAL USE ONLY

FOR OFFICIAL USE ONLY

$$\left. \begin{aligned} \bar{A}_m \alpha_1 + \bar{A}_m^* \alpha_1^* + \frac{\epsilon_2}{\epsilon_1} \sum_{n=1}^{\infty} (\bar{B}_n + \bar{B}_n^*) J_1^{mn} &= \frac{\epsilon_2}{\epsilon_1} U_{m1} \\ \bar{B}_n \beta_1 + \bar{B}_n^* \beta_1^* + \frac{\epsilon_2}{\epsilon_3} \sum_{m=1}^{\infty} (\bar{A}_m + \bar{A}_m^*) K_1^{nm} &= \frac{\epsilon_2}{\epsilon_3} U_{n1} \end{aligned} \right\},$$

(1)

where

$$\begin{aligned} \bar{A}_m &= A_m \operatorname{ch} \frac{\pi m}{d_2} a_1; \quad \bar{A}_m^* = A_m^* \operatorname{sh} \frac{\pi m}{d_3} a_1; \quad \bar{B}_n = B_n \operatorname{ch} \frac{\pi n}{d_1} b_1; \\ \bar{B}_n^* &= B_n^* \operatorname{sh} \frac{\pi n}{d_1} b_1; \quad \alpha_1 = \operatorname{th} \frac{\pi m}{d_2} a_1 + \frac{\epsilon_2}{\epsilon_1} \operatorname{cth} \frac{\pi m}{d_1} a_1; \quad \alpha_1^* = \operatorname{cth} \frac{\pi m}{d_2} a_1 + \\ &+ \frac{\epsilon_2}{\epsilon_1} \operatorname{cth} \frac{\pi m}{d_2} a_1; \quad \beta_1 = \operatorname{th} \frac{\pi n}{d_1} b_1 + \frac{\epsilon_2}{\epsilon_3} \operatorname{cth} \frac{\pi n}{d_1} b_1; \quad \beta_1^* = \operatorname{cth} \frac{\pi n}{d_1} b_1 + \\ &+ \frac{\epsilon_2}{\epsilon_3} \operatorname{cth} \frac{\pi n}{d_1} b_1; \quad J_1^{mn} = \frac{2}{d_1} \frac{n}{m} \frac{\cos \pi m}{\operatorname{sh} \frac{\pi n}{d_1} d_2} \int_{b_1}^{b_2} \operatorname{sh} \frac{\pi n}{d_1} (b_2 - y) \sin \frac{\pi m}{d_2} (b_2 - y) dy = - \\ &= - \frac{2 \frac{\pi n}{d_1} \cos \pi m \cos \pi n}{\left(\frac{\pi m}{d_2}\right)^2 + \left(\frac{\pi n}{d_1}\right)^2}; \end{aligned}$$

$$\begin{aligned} K_1^{nm} &= \frac{2}{d_2} \frac{m}{n} \frac{\cos \pi n}{\operatorname{sh} \frac{\pi m}{d_2} d_1} \int_{a_1}^{a_2} \operatorname{sh} \frac{\pi m}{d_2} (a_2 - x) \sin \frac{\pi n}{d_1} (a_2 - x) dx = \\ &= - \frac{2 \frac{\pi m}{d_2} \cos \pi n \cos \pi m}{\left(\frac{\pi m}{d_2}\right)^2 + \left(\frac{\pi n}{d_1}\right)^2}; \end{aligned}$$

FOR OFFICIAL USE ONLY

FOR OFFICIAL USE ONLY

$$U_{m1} = -\frac{2U_0}{\pi m d_1 d_2} \int_{b_1}^{b_2} (y - b_2) \sin \frac{\pi m}{d_2} (y - b_2) dy = \frac{2U_0}{(\pi m)^2} \frac{d_2}{d_1} \cos \pi m;$$

$$U_{n1} = -\frac{2U_0}{\pi n d_1 d_2} \int_{a_1}^{a_2} (x - a_2) \sin \frac{\pi n}{d_1} (x - a_2) dx = \frac{2U_0}{(\pi n)^2} \frac{d_2}{d_1} \cos \pi n.$$

Systems of equations from boundary conditions in other quadrants are arrived at from (1) by the substitutions:

For the second quadrant:

$$a_2 \rightarrow \bar{a}_2, \quad e_2 \rightarrow e'_2, \quad e_3 \rightarrow e'_3, \quad \bar{B}_n \rightarrow \bar{F}_1, \quad \bar{B}_n^* \rightarrow \bar{F}_1^*, \quad \bar{A}_m^* \rightarrow -\bar{A}_m;$$

For the third quadrant:

$$a_2 \rightarrow \bar{a}_2, \quad e_2 \rightarrow e'_2, \quad e_3 \rightarrow e'_3, \quad \bar{B}_n \rightarrow \bar{F}_1, \quad \bar{B}_n^* \rightarrow -\bar{F}_1^*,$$

$$\bar{A}_m \rightarrow \bar{E}_k, \quad \bar{A}_m^* \rightarrow \bar{E}_k^*, \quad b_2 \rightarrow \bar{b}_2, \quad e_1 \rightarrow e'_1; \quad (2)$$

For the fourth quadrant:

$$b_2 \rightarrow \bar{b}_2, \quad e_2 \rightarrow e''_2, \quad e_1 \rightarrow e'_1, \quad \bar{B}_n^* \rightarrow -\bar{B}_n^*, \quad \bar{A}_m \rightarrow \bar{E}_k;$$

$$\bar{A}_m^* \rightarrow -\bar{E}_k^*. \quad (2)$$

We solve the general system of equations by the reduction method upon condition of equality of individual amplitude factors in adjacent (in relation to quadrants) partial regions, which corresponds to fulfillment of boundary conditions for tangential components of the electromagnetic field at the limits of $x = 0$ and $y = 0$.

Solutions of the system (amplitude factors) are used for finding unit-length parameters of the line under consideration (capacitance and wave impedance), the equations for the calculation of which are arrived at on the basis of the relationships:

$$C = \left[-\epsilon \int_S E_n ds \right] \frac{1}{U}; \quad W = \sqrt{\frac{\mu}{\epsilon}} \frac{e}{C}, \quad (3)$$

FOR OFFICIAL USE ONLY

FOR OFFICIAL USE ONLY

where s is the surface of a unit of length of the line's outer conductor; E_n is the electric field component normal to S ; and U is the difference in potential between conductors.

The equation for calculating unit-length capacitance characteristic of the first quadrant of the line's cross section (fig 1a), arrived at by integration in (3) in terms of the surface of the outer conductor, has the form:

$$\begin{aligned}
 C_1 &= C_{11} + C_{12} + C_{13}; \\
 C_{11} &= \epsilon_1 \left\{ \frac{a_1}{d_2} + \sum_{m=1}^{\infty} \left[\bar{A}_m \operatorname{th} \frac{\pi m}{d_2} a_1 + \bar{A}_m^* \left(\operatorname{cth} \frac{\pi m}{d_2} a_1 - \frac{1}{\operatorname{sh} \frac{\pi m}{d_2} a_1} \right) \right] \right\}; \\
 C_{12} &= \epsilon_2 \left\{ \frac{1}{2} \left(\frac{d_1}{d_2} + \frac{d_2}{d_1} \right) + \sum_{m=1}^{\infty} (\bar{A}_m + \bar{A}_m^*) \left(\operatorname{cth} \frac{\pi m}{d_2} d_1 - \frac{\cos \pi m}{\operatorname{sh} \frac{\pi m}{d_2} d_1} \right) + \right. \\
 &\quad \left. + \sum_{n=1}^{\infty} (\bar{B}_n + \bar{B}_n^*) \left(\operatorname{cth} \frac{\pi n}{d_1} d_2 - \frac{\cos \pi n}{\operatorname{sh} \frac{\pi n}{d_1} d_2} \right) \right\}; \\
 C_{13} &= \epsilon_3 \left\{ \frac{b_1}{d_1} + \sum_{n=1}^{\infty} \left[\bar{B}_n \operatorname{th} \frac{\pi n}{d_1} b_1 + \bar{B}_n^* \left(\operatorname{cth} \frac{\pi n}{d_1} b_1 - \frac{1}{\operatorname{sh} \frac{\pi n}{d_1} b_1} \right) \right] \right\}.
 \end{aligned}
 \tag{4}$$

Similar in appearance are the equations for calculating the unit-length capacitance of the remaining quadrants (C_2 , C_3 and C_4). They are arrived at from (4) by substitutions in (2). Summation of these capacitances gives the total capacitance of the line. The equation for the wave impedance characteristic of the first quadrant will be

$$\frac{1}{W_1} = \sqrt{\frac{\epsilon_1}{\mu}} \frac{C_{11}}{\epsilon_1} + \sqrt{\frac{\epsilon_2}{\mu}} \frac{C_{12}}{\epsilon_2} + \sqrt{\frac{\epsilon_3}{\mu}} \frac{C_{13}}{\epsilon_3}.$$

FOR OFFICIAL USE ONLY

FOR OFFICIAL USE ONLY

The values of W_2 , W_3 and W_4 for the remaining quadrants are determined by means of (2). The total wave impedance of the line is computed thus:
 $1/W = 1/W_1 + 1/W_2 + 1/W_3 + 1/W_4$.

For the purpose of analyzing the agreement of solutions and the accuracy provided by this algorithm, detailed numerical investigations were made for the case of a uniformly filled line with a symmetrically arranged inner conductor. Here the systems of equations for individual quadrants proved to be identical and in calculations was employed only system (1), where $\bar{A}_m^* = \bar{B}_n^* = 0$, $\epsilon_1 = \epsilon_2 = \epsilon_3 = 1.0$, and $m = n$.

The results of an investigation of the agreement of solutions are given in fig 2, where curve C_1 corresponds to a calculation of capacitance in terms of a unit-length charge on the surface of the inner conductor and curve C_2 in terms of a charge on the surface of the line's outer conductor. For the purpose of analyzing the accuracy of the algorithm, the calculated values of W were compared with the results of [1,2] arrived at by means of the method of conformal transformations (these results can be regarded as precise), as well as with values arrived at by other methods [3,4]. The dependence of the integral characteristic ($C/4\epsilon$) of the line on the number, N , of the approximation (fig 2) testifies to the good uniform agreement of solutions; the results arrived at by means of this algorithm practically do not change when $N \geq 10$. It is obvious from this figure that in integrating for the surface of an outer conductor not containing singular points, the unit-length capacitance rapidly approaches (curve C_2) the precise value of [1] even in the case of a very thin inner conductor. The second dependence (curve C_1) shows considerably worse agreement of the results with the precise values.

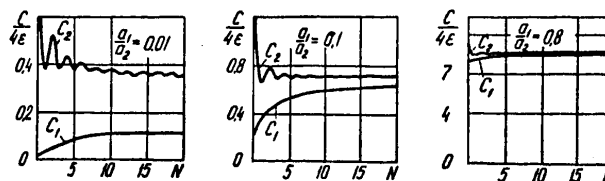


Figure 2.

A detailed comparison (tables 1 and 2) of the results arrived at by means of the algorithm suggested with the precise values [1,2] demonstrates their good agreement with any geometrical parameters of the conductors.

In table 1 are given also the results arrived at in [3] by the net-point method by using 60 horizontal divisions in a net. From comparing these with the precise values, we see that even in such a high approximation the

FOR OFFICIAL USE ONLY

FOR OFFICIAL USE ONLY

net-point method is considerably inferior in accuracy to the algorithm suggested. In the same table are given the results arrived at in a 20-th approximation based on the procedure in [4]. The approximation number agrees with that in which the authors' results presented in the table were arrived at.

Table 1.

a_1/a_2	1) Ω , Ом точно Вовтор	2) Ω , Ом дан- ный алго- ритм	$ \Delta\Omega $, %	3) Ω , Ом графиков [3]	$ \Delta\Omega $, %	4) Ω , Ом по методике [4]	$ \Delta\Omega $, %
0,01	270,69	260,70	3,69	—	—	273,39	0,99
0,1	132,65	132,1	0,41	—	—	134,86	1,67
0,2	91,11	90,94	0,19	92,0	0,98	105,58	15,88
0,3	66,87	66,81	0,09	67,5	0,94	73,68	10,18
0,4	49,82	49,79	0,06	50,5	1,37	58,08	16,58
0,5	36,81	36,80	0,03	37,0	0,52	45,82	24,48

Key:

1. Ω , precise
2. Ω , our algorithm
3. Ω , graphs in [3]

4. Ω , according to procedure in [4]

Table 2.

a_1/b_1	a_2/b_2	b_1/b_2	1) Ω , Ом дан- ный алго- ритм	2) Ω , Ом [2]
0,30594	0,30594	0,4	49,97	50,0
0,20398	0,79168	0,4	59,87	60,0
0,06666	0,60036	0,4	67,90	68,0

Key:

1. Ω , our algorithm
2. Ω , in [2]

From table 1 it is obvious in addition that the results of study [4] differ considerably from the precise values, which can be explained by a certain incorrectness in formulation of the problem: In describing the field in the side region, the term of the series was not taken into account which provides for a fixed difference in potential between the line's conductors, and the unit-length capacitance was calculated in terms of the charge in the line's inner conductor. The data from [1,2] presented above were

FOR OFFICIAL USE ONLY

arrived at with precise equations, but it must be mentioned that for the purpose of practical use these equations are rather cumbersome (they contain elliptic integrals of the first kind), they do not make it possible efficiently to calculate the distribution of the field in terms of the line's transverse section, and are suitable only for the calculation of rectangular lines with symmetrically arranged conductors.

The algorithm suggested is free of these disadvantages and ensures high precision of the solution (tables 1 and 2) with a relatively not too great number of computations. Calculation of one variant of a line on a BESM-4M computer (the program is written in the algorithmic language Fortran-20) takes on the order of 90 s.

Based on the algorithm suggested, it is possible to construct calculation equations for more complex (fig 1b, c and d) band lines in a quasi-T approximation. If it is taken into account that along axis of symmetry AB in fig 1b, c and d the conditions of an electrical wall are fulfilled (with excitation of odd parity), the line can be regarded as two individual lines, the procedure for the calculation of which is presented above. In a similar manner are calculated the unit-length parameters of the lines in fig 1b, c and d with even-parity excitation. In this case Hertz vectors in partial regions of the first quadrant of the line's cross section (fig 1a) are written in the form:

$$\begin{aligned}\Pi_{z1}^e &= \left\{ U_0 \frac{b_2 - y}{d_2} + \sum_{m=1}^{\infty} \left(A_m \operatorname{ch} \frac{\pi m}{d_2} x + A_m^* \operatorname{sh} \frac{\pi m}{d_2} x \right) \times \right. \\ &\quad \left. \times \sin \frac{\pi m}{d_2} (b_2 - y) \right\} e^{-i\omega \sqrt{\epsilon_3 \mu_2} z}; \\ \Pi_{z2}^e &= \left\{ U_0 \frac{b_2 - y}{d_2} + \sum_{m=1}^{\infty} C_m \sin \frac{\pi m}{d_2} (b_2 - y) \operatorname{sh} \frac{\pi m}{d_2} (a_2 - x) + \right. \\ &\quad \left. + \sum_{n=1}^{\infty} D_n \cos \frac{\pi n}{2d_1} (a_2 - x) \operatorname{sh} \frac{\pi n}{2d_1} (b_2 - y) \right\} e^{-i\omega \sqrt{\epsilon_3 \mu_2} z}; \\ \Pi_{z3}^e &= \left\{ U_0 + \sum_{n=1}^{\infty} \left(B_n \operatorname{ch} \frac{\pi n}{2d_1} y + B_n^* \operatorname{sh} \frac{\pi n}{2d_1} y \right) \times \right. \\ &\quad \left. \times \cos \frac{\pi n}{2d_1} (a_2 - x) \right\} e^{-i\omega \sqrt{\epsilon_3 \mu_2} z}; \\ m &= 1, 2, \dots, n = 1, 3, 5, \dots\end{aligned}$$

FOR OFFICIAL USE ONLY

FOR OFFICIAL USE ONLY

After writing boundary conditions with $x = a_1$ and $y = b_1$, it is possible to arrive at equations similar to (1). Also constructed is a system of equations for the fourth quadrant. The total system of equations is arrived at by a combination of the system for the first and fourth quadrants with the boundary condition when $x = a_2$ conforming to a magnetic wall, and for the second and third quadrants with boundary conditions for $x = -a_2$ conforming to an electrical wall.

Bibliography

1. Bowman, F. "Introduction to Elliptic Functions," Dover, New York, 1961.
2. Biblet, H.J. "The Exact Dimensions of a Family of Rectangular Coaxial Lines with Given Impedance," IEEE TRANS., 1972, MTT-20, N 8, pp 538-541.
3. Metcalf, W.S. "Characteristic Impedance of Rectangular Transmission Lines," PIRE, 1965, 112, N 11, pp 2033-2039.
4. Bräckelmann, W. "Wellentypen auf der Streifenleitung mit rechteckigem Schirm" [Wave Types in a Strip Conductor with a Rectangular Shield], AEU, 1967, 21, No 12, pp 641-648.

COPYRIGHT: IZVESTIYA VUZOV SSSR, RADIOELEKTRONIKA, 1979
[53-8831]

CSO: 1860
8831

FOR OFFICIAL USE ONLY

FOR OFFICIAL USE ONLY

Electromagnetic Wave Propagation

UDC: 621.371.25

SCATTERING OF MODES OF THE WHISPERING GALLERY TYPE BY IONOSPHERIC
INHOMOGENEITIES ALONG A GEOMAGNETIC FIELD

Moscow IZVESTIYA VYSSHIKH UCHEBNIK ZAVEDENIY: RADIOFIZIKA in Russian No 10
Vol 22 1979 pp 1195-1204

[Article by A. F. Belenov and Yu. V. Chugunov]

[Text] This article examines scattering of modes of the whispering gallery type by inhomogeneities extended along a geomagnetic field. Coefficients of mode excitation are calculated with scattering of one mode into another and with scattering of a plane wave by an extended inhomogeneity (analog of "angular" scattering in a geometrical-optics approximation). Problems of mode selection in such scattering are discussed.

As we know [1-4], ionospheric waveguides (IVK) can be excited due to the inhomogeneous structure of the dielectric constant of the ionospheric plasma. Many studies have been dedicated to this question. For example, the authors of [2] developed adiabatic theory of capture of radio waves in IVK due to refraction on regular horizontal ionospheric discontinuities, while the authors of [4] solve a problem in approximation of geometrical optics on excitation of IVK as a result of scattering of radio waves on random inhomogeneities of the ionosphere; the authors of [3] discuss the results of a waveguide approach to the problem of the effect of inhomogeneities of ionospheric plasma on the spectrum of natural modes of IVK.

In this article we shall examine the problem of excitation of whispering gallery type modes in IVK [6]. Principal attention is focused on waveguide excitation by scattering on inhomogeneities extended along a geomagnetic field. It is demonstrated how anisotropy of inhomogeneities influences conditions of most optimal "washing down" of IVK. At the same time we shall note that scattering of radio waves by isotropic inhomogeneities in IVK was examined in [9].

1. We shall represent an IVK containing inhomogeneities in the form of a homogeneous and inhomogeneous part. The model of the homogeneous portion

FOR OFFICIAL USE ONLY

FOR OFFICIAL USE ONLY

of the waveguide here was selected in the form of a cylindrical cavity with $\epsilon = 1$ when $r < R_1$ and $\epsilon = \epsilon_1 < 1$ when $r \geq R_1$ (ϵ -- dielectric constant of the layer, r -- distance to point of observation in a cylindrical coordinate system with the origin at the earth's center). Waveguide parameters -- volume of waveguide channel, number of modes in the channel, volume occupied by the individual mode -- depend on selection of quantities R_1 and ϵ_1 . On the basis of the analysis of round-the-world propagation of short radio waves performed in [1], one can select quantities ϵ_1 and R_1 so that the above-listed parameters of the waveguide model under consideration are close to the analogous parameters of an actual above-ground waveguide. For the frequency band $\omega \cdot (1.5-2) \times 10^8$ Hz one should assume $\epsilon_1 = 0.92$, $z_1 = 90$ km (day), where $z_1 = R_1 - R_0$; R_0 -- earth's radius, and $\epsilon_1 = 0.92$, $z_1 = 100$ km (night). The selected parameters satisfactorily describe propagation of radio waves in the plane of a great circle in this model.

We shall specify the inhomogeneous portion of the waveguide in the form of an axisymmetric disturbance of the dielectric constant:

$$\epsilon_{11} = 1 - \Delta\epsilon(x, z).$$

Cartesian coordinate system x, z (see Figure 1) is placed in such a manner that the axis of symmetry of the inhomogeneity coincides with the z axis. Let us examine disturbance of an ionospheric waveguide due to scattering of an incident electromagnetic wave with amplitude of electric field E_{inc}^1 on inhomogeneity $\Delta\epsilon(x, z)$. When $\Delta\epsilon \ll 1$ density of flux excited by the incident wave can be written in the form²

$$j(x, z) = i\omega \Delta\epsilon(x, z) E_{\text{inc}}^1. \quad (1)$$

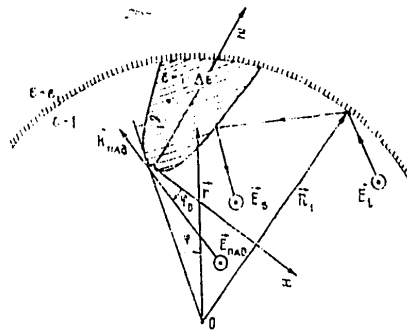


Figure 1.

We shall represent the scattered field in the form of superposition of waveguide natural modes

$$E_p = \sum_l (D_l E_l + D_{-l} E_{-l}), \quad (2)$$

FOR OFFICIAL USE ONLY

where E_{+L} is a set of functions comprising the natural modes of an ionospheric waveguide. In the considered case of a cylindrical cavity for horizontal wave polarization (when vector E_{+L} is parallel to the axis of the cylinder), expressions for E_{+L} are well known [5]:

$$E_{+L} = y_0 \exp(-i v_L z) \begin{cases} H_{v_L}^{(2)}(k_0 \sqrt{\epsilon_1} r) & (r > R_1) \\ J_{v_L}(k_0 r) & (r < R_1) \end{cases} \quad (3)$$

Here y_0 is a unit vector parallel to the axis of the cylinder; r, φ -- polar coordinates in the plane of a great circle,

$J_L(\tau), H_L^{(2)}(\tau)$ -- Bessel functions of the first and second kind,

$k_0 = \omega/c, v_L \approx k_0 R_1$ $M_L, M_L = (k_0 R_1/2)^{1/3}$, where t_L is the L root of Airy function $v(-t_L), t, e, v(-t_L) = 0$.

Coefficient of excitation D_{+L} of mode number L is linked with the current exciting diffraction modes by relation [5]

$$D_{+L} = -\frac{1}{N_L} \iint_V E_{+L} j(x, z) dx dz, \quad (4)$$

where

$$N_L = \int_{R_1}^{\infty} \frac{\epsilon_0}{\epsilon_1} \frac{R_1}{r} |H_{v_L}^{(2)}(k_0 \sqrt{\epsilon_1} R_1)|^2, \quad (5)$$

integration is performed on the volume occupied by the inhomogeneity. Expressions (2), (3) and (5) make it possible to calculate coefficients of excitation D_{+L} of waveguide modes with scattering by an inhomogeneity located in a waveguide channel.

2. Let us examine the case where an incident wave is one of the natural modes of an ionospheric waveguide, that is, $E_{+L} = E_S$.

Utilizing Langer-(Fok) uniform asymptotic behavior [7] for $J_{v_L}(\tau)$ when $v \gg 1, v \sim \tau$, from (1), (3), (5) under condition $L_x \sin \alpha_0 \ll (1/3)(k_0^{-2} R_0)^{1/3}$ we obtain (L_x -- characteristic scale of an inhomogeneity across a geomagnetic field, α_0 -- geomagnetic field angle of inclination³)

$$D_{+L} = Q I, \quad (6)$$

$$Q = \frac{i \omega \epsilon_0}{\pi N_L M^2} \frac{H_{v_L}^{(2)}(k_0 \sqrt{\epsilon_1} R_1) H_{v_S}^{(2)}(k_0 \sqrt{\epsilon_1} R_1)}{J_{v_L}(k_0 R_1) J_{v_S}(k_0 R_1)},$$

$$I = \int_0^{L_x} \tilde{\Delta}_z(x, z) \exp \left[i \left(v_e - v_s \right) \frac{z \sin \alpha_0}{R_1} \right] v(z) v(z_s) dz.$$

FOR OFFICIAL USE ONLY

FOR OFFICIAL USE ONLY

Here

$$\xi_{l,s} = [v_{l,s} - k_n(R_1 - L_z \cos \alpha_0 + z \cos \alpha_0)] \frac{1}{M},$$

$$\tilde{\Delta}_\varepsilon(x, z) = \int_{-\infty}^{+\infty} \Delta_\varepsilon(x, z) e^{ik_x x} dx, \quad x = \frac{\cos \alpha_0}{R_1} (v_l - v_s),$$

a plus sign corresponds to forward scatter, a minus sign to backscattering, and L_z -- dimension of inhomogeneity on the z axis.

In the case of forward scattering integral I, standing on the right-hand side of (6), when $L_z \gg L_{E_\perp} / \cos \alpha_0$ is equal to

$$I \approx \tilde{\Delta}_\varepsilon(x) \int_0^{L_z} v(\xi_l) v(\xi_s) dz. \quad (7)$$

The region essential for integration in (7) is determined by waveguide channel volume for the mode with the smallest subscript. As is evident from (7), the largest value of excitation coefficient for forward scattering is attained when $l \sim s$. In this case

$$D_{l,s} \sim Q \tilde{\Delta}_\varepsilon(x) \frac{M}{k_0 \cos \alpha_0}. \quad (8)$$

The situation is somewhat more complicated for backscattering, since it is necessary to take account of phase factor $\exp(i v_l \phi)$. For example, when

$$s \sim 1, L_z \gg (L_{E_\perp}, t_l \cos \alpha_0) = L_{E_l}$$

the coefficient of excitation is equal to

$$D_{l,1} \approx Q \int_0^{L_z} \tilde{\Delta}_\varepsilon(x, z) v(\xi_l) v(\xi_1) \exp(2ik_0 z \sin \alpha_0) dz. \quad (9)$$

The integral on the right-hand side of (9) can be computed by the stationary phase method:

$$D_{l,1} \approx \tilde{\Delta}_\varepsilon(x, z_{CT}) Q \frac{M}{\sqrt{\pi} t_l^{1/4} k_0 \cos \alpha_0} v(\xi_l(z_{CT})), \quad (10)$$

where stationary point z_{CT} is determined by expression

$$t_l = \frac{k_0}{M} \cos \alpha_0 (L_z - z_{CT}) = M^2 \tan^2 \alpha_0. \quad (11)$$

Thus a contribution to backscattering is made by modes for which the stationary point falls within integration interval $(0, L_z)$. Scattering takes place into modes which differ greatly from incident $l \gg s$, and condition (11) is the analog of "angular" condition with scattering of a plane wave in a vacuum by extended inhomogeneities [8].

We shall estimate the fraction of scattered energy for the case of incidence of "glancing" wave⁴ ($s \sim 1$) on an inhomogeneity. Let Δn be

FOR OFFICIAL USE ONLY

FOR OFFICIAL USE ONLY

characteristic number of scattered modes, l -- number of mode with the largest coefficient of excitation. A general expression for fraction of scattered energy has the form

$$W_{p,l,s} \sim \Delta n |D_{l,s}|^2 \frac{L_{l,l}}{L_{l,s}} \left| \frac{H_{l,l}^{(2)}(k_0 \sqrt{\epsilon_1} R_1) J_{l,s}(k_0 R_1)}{H_{l,s}^{(2)}(k_0 \sqrt{\epsilon_1} R_1) J_{l,l}(k_0 R_1)} \right|^2. \quad (12)$$

An estimate of the fraction of energy withdrawn from the waveguide channel and incident on the earth's surface is evidently of the greatest interest. For modes where the lower caustic touches the earth's surface,

$l \sim 3 \cdot 10^2$, $\Delta n \sim 3$. For a quantitative estimate of the expression in the right-hand part of (12) we shall utilize expression (5) for N_l , as well as asymptotic form $J_{\nu_l}(k_0 R_1)^5$

$$W_{-l,s} \approx \frac{3}{\pi} \frac{\Delta \epsilon_{\max}^2}{\cos^4 \alpha_0} t_{300}^{-1/2} = \left(\frac{\Delta \epsilon_{\max}}{2 \cos^2 \alpha_0} \right)^2 \frac{12}{\pi t_{300}^2}. \quad (13)$$

The quantity in parentheses in (13) is the Fresnel coefficient of reflection from a plane-parallel plate $h_0/2 \cos \alpha_0$ in thickness with dielectric constant $1 - \Delta \epsilon_{\max}$. Thus the fraction of energy scattered by an inhomogeneity in a supraterrrestrial channel for the case of wave incidence angles satisfying conditions of scattered signal striking the earth, obtained with the aid of a wave approach, differs from the results of an analogous problem solved by the method of geometrical optics by factor

$$12/\pi t_{300}^2 \sim 1/3.$$

A decrease in the fraction of scattered energy in comparison with the fraction calculated in a geometrical optics approximation can be explained by a qualitative difference in structure of the field of plane waves. When a waveguide mode strikes an inhomogeneity, one must take account of the structure of the field in the vicinity of the caustic curve, which can be done within the framework of the employed wave approach.

The principal results of this section can be formulated as follows.

1) With direct scattering on an inhomogeneity extending along a magnetic field, waveguide mode is transformed into modes close to incident mode.

2) With backscattering modes satisfying relation (11), which is a wave analog of conditions of geometric aspect, are excited most effectively [8].

3) Conditions of scattering of a mode with $l \sim 1$ into modes with $l \gg 1$, the lower caustic curve of which touches the earth's surface, depend on the transverse dimension of the channel and angle of inclination α_0 of the inhomogeneity to the vertical. For a channel with the smallest

FOR OFFICIAL USE ONLY

FOR OFFICIAL USE ONLY

lateral dimensions, such scattering is most effective when

$$\alpha_0 \sim \arctg [H_0^2 / (k_0 R_1)^3] \sim 15^\circ.$$

The fraction of energy scattered from the channel comprises 0.01% of the energy contained in the mode incident on the inhomogeneity.

3. We shall now examine excitation of an IVK by a radio signal radiated from the earth's surface. Let the wave vector of the radio wave emitted by the transmitter and incident on the inhomogeneity comprise angle φ_0 with the x axis (see Figure 1):

$$E_{\text{inc}} = y_0 E_0 \exp(-ik_0 z \sin \varphi_0 + ik_0 x \cos \varphi_0). \quad (14)$$

Substituting an expression for E_{inc} in relations (3)-(5), which define coefficient $D_{\pm l}$ of excitation of waveguide modes, we obtain

$$D_{\pm l} = \frac{i \omega \varepsilon_0 E_0 H_l^{(2)}(k_0 \sqrt{\varepsilon_1} R_1)}{\sqrt{\pi} N_l M J_{\gamma_l}(k_0 R_1)} \int_0^{L_z} \widetilde{\Delta \varepsilon}(x, z) v(\xi_l) \exp(i \gamma_l z) dz, \quad (15)$$

where

$$\begin{aligned} \widetilde{\Delta \varepsilon}(x, z) &= \int_{-\infty}^{+\infty} \Delta \varepsilon(x, z) e^{i \gamma x} dx, \\ x &= k_0 \left(\cos \varphi_0 + \frac{y_l}{k_0 R_1} \cos \alpha_0 \right), \\ \gamma &= -k_0 \left(\sin \varphi_0 + \frac{y_l}{k_0 R_1} \sin \alpha_0 \right), \\ \xi_l &= (y_l + k_0 [R_1 + (z - L_z) \cos \alpha_0]) \frac{1}{M}, \\ M &= \left(\frac{k_0 R_1}{2} \right)^{1/3}. \end{aligned}$$

In the case of direct scattering, the region important for integration in (15) is determined by term $e^{i \gamma x}$:

$$|D_{\pm l}| \approx \widetilde{Q} \widetilde{\Delta \varepsilon}(x, 0) \frac{v(\xi_l(0))}{\gamma}. \quad (16)$$

Here

$$\widetilde{Q} = \frac{\omega \varepsilon_0 H_l^{(2)}(k_0 \sqrt{\varepsilon_1} R_1)}{\sqrt{\pi} N_l M J_{\gamma_l}(k_0 R_1)}.$$

Expression (16) shows that excitation of waveguide modes during direct scattering is negligibly small in view of the smallness of term

$$\widetilde{\Delta \varepsilon}(x, 0).$$

FOR OFFICIAL USE ONLY

FOR OFFICIAL USE ONLY

In fact, in this instance the scattering diagram is greatly extended in a direction comprising with the interface an angle which exceeds the angle of full internal reflection, and only a small fraction of the energy scattered in a direction close to the direction of vector k_0 is "captured" into the canal.

With backscattering factor $e^{i\gamma z}$, which stands under the sign of the integral in (15), can be sufficiently slow, and therefore it is necessary to take account of change in function $v(\xi, z)$, which describes the transverse structure of the waveguide mode. For modes the waveguide channel of which has least transverse dimensions $l \sim 1$, at angles of incidence φ_0 which satisfy condition

$$\frac{2\pi}{k_n \left(\sin z_0 - \frac{v_l}{k_n R_l} \sin z_0 \right)} \sim \frac{l \cdot E_1}{\cos z_n}, \quad (17)$$

a change in factor $e^{i\gamma z}$ under the integral in (15) can be ignored. In this case when $L_z \gg M/k_0 \cos \alpha_0$, $L_x \sim \lambda_0/2 \cos \alpha_0$ the coefficient of excitation is equal to

$$|D_{-l}| \approx \tilde{Q} \Delta \varepsilon_{\max} \frac{M}{2k_0^2 \cos^2 z_n}, \quad (18)$$

where $\Delta \varepsilon_{\max}$ -- maximum deviation of dielectric constant from $\varepsilon = 1$ in the inhomogeneity.

For angles φ_0 which greatly differ from α_0 ,

$$\frac{2\pi}{k_n \left| \sin z_0 - \frac{v_l}{k_n R_l} \sin z_n \right|} \sim \frac{l \cdot E_1}{\cos z_n}, \quad (19)$$

an expression for D_{-l} can be obtained in the same manner as in the case of direct scattering, namely:

$$|D_{-l}| \approx \frac{\tilde{Q} \Delta \varepsilon(x, 0) v(\xi_l(0))}{\gamma}. \quad (20)$$

In this case (condition (19)) excitation of waveguide modes, just as for direct scattering, is negligibly small. Comparing results (18) and (20), one can conclude that excitation of waveguide modes with $l \sim 1$ is substantial at angles of incidence φ_0 lying within the range

$$|z_n - z_0| \lesssim \frac{1}{M}. \quad (21)$$

FOR OFFICIAL USE ONLY

FOR OFFICIAL USE ONLY

At magnetic field angles of inclination corresponding to middle latitudes ($\alpha_0 \sim 20^\circ$), condition (21) gives $19.5 \leq \varphi_0 \leq 20.5$ the fraction of energy captured into the waveguide channel is determined approximately by characteristic number Δn of modes for which the coefficient of excitation with specified φ_0 and α_0 coincides in order of magnitude with $D_{l\max}$. As will be shown below, the above considerations are correct for waveguide modes with $l \lesssim 3$. Determining the fraction of captured energy \tilde{W}_p in a manner analogous to the above, we obtain the following for angles φ_0 and α_0 which satisfy relation (21):

$$\tilde{W}_p \approx 3(\Delta \varepsilon_{\max})^2. \quad (22)$$

We shall now examine conditions of excitement of waveguide modes with $l \gg 1$. Utilizing to compute the integral in the right-hand part of (15) Airy function asymptotic form [7]:

$$v(\xi) \sim \xi^{-1/4} \sin \left[\frac{2}{3} \xi^{3/2} + \frac{\pi}{4} \right], \quad (23)$$

and computing the given interval by the stationary phase method, we obtain

$$|D_{-l}| \approx \frac{\tilde{Q} M \tilde{\Delta \varepsilon}(x, z)}{k_0 \cos \alpha_0}. \quad (24)$$

Stationary point z_1 in expression (24) satisfies relation

$$\tilde{\varepsilon}_l(z_1) = \left(\frac{\tilde{Q} M}{k_0 \cos \alpha_0} \right)^2. \quad (25)$$

Expression (24) applies with angles of incidence φ_0 satisfying condition⁶

$$\frac{M l_l}{k_0 R_1} \leq |\varphi_0 - \alpha_0| \leq \frac{\sqrt{l_l}}{M}. \quad (26)$$

Curves of relationship between coefficient of excitation $|D_{-l}|$ and angle of incidence φ_0 with a specified α_0 are qualitatively represented in Figure 2. In finding the relationship between $|D_{-l}|$ and φ_0 we utilized relation

$$\tilde{\Delta \varepsilon}(x, z) \approx \Delta \varepsilon_{\max} \pi x,$$

obtained from (25). On the basis of (18), (24) and conditions (19) and (26), we plotted the above-indicated curves with $l \sim 1$ (curve 1), $l \sim 10$ (curve 2) and $l \sim 10^2$ (curve 3). One can draw the following conclusions from analysis of curves D_{-l} , contained in Figure 2.

FOR OFFICIAL USE ONLY

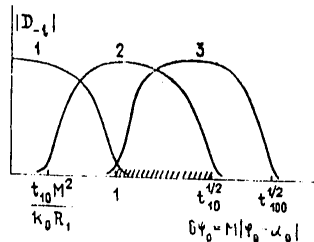


Figure 2.

1) In the range of angles of incidence satisfying relation (21), modes with the least transverse dimension $L_{E1} \sim M/k_0$ are most effectively excited.

2) In the range of angles of incidence

$$\frac{1}{M} \leq |\varphi_0 - \alpha_0| \leq \frac{\sqrt{t_{10}}}{M} \quad (27)$$

a maximum number of modes $\Delta n_{\max} \sim 10^2$ is excited, that is, the entire spectrum of waveguide modes.

3) Modes with the largest transverse dimension $L_{E\max} \approx Mt_{100}/k_0$ are excited in range of angles of incidence

$$\frac{1}{M} \leq |\varphi_0 - \alpha_0| \leq \frac{\sqrt{t_{100}}}{M} \quad (28)$$

It follows from this that the maximum fraction of captured energy

$$\tilde{W}_{p_{\max}} \approx 10^2 (\Delta \varepsilon_{\max})^2 \quad (29)$$

will be excited in a supraterritorial waveguide at inhomogeneity angles of incidence satisfying condition (27). When

$$\varphi_0 \sim 20^\circ, \quad \Delta \varepsilon \sim 10^{-2}$$

captured energy comprises 1% of energy incident on the inhomogeneity at angles of incidence φ_0 , deviating from angles satisfying the condition of geometrical aspect of not more than $1^\circ.6$ and not less than $0^\circ.56$.

We assumed that the inhomogeneity covers the entire volume of the waveguide channel. With a decrease in dimensions of the inhomogeneity to quantity $L_{E1}/\cos \alpha_0$, the conclusions reached in this section pertaining to excitation of a mode with $l \sim 1$ remain in force.

FOR OFFICIAL USE ONLY

FOR OFFICIAL USE ONLY

The maximum fraction of captured energy decreases thereby approximately 10-fold, since the maximum possible number of excited modes decreases to an equal degree. That inhomogeneity position which is energetically most advantageous for excitation of a supraterrrestrial waveguide will be achieved along the channel lower boundary, satisfying $l \sim 10$, that is, at a distance of Mt_{10}/k_0 from the upper boundary of the supraterrrestrial waveguide.⁷ The region of angles of incidence for a given inhomogeneity position, just as in the case

$$L_z \cos \alpha_0 > L_{F_{10}},$$

is determined by condition (27).

Let us compare the magnitude of the fraction of energy \tilde{W}_p captured in a waveguide channel (capture coefficient) determined by relation (29), with capture coefficient value G_0 , obtained in a geometrical optics approximation ([10], page 39). Applied to the above-considered two-dimensional case for inhomogeneities with dimensions $L_x \ll k_0^{-1}$, the ratio of these capture coefficients comprises $\tilde{W}_p/G_0 \sim 10^2$. The fact that \tilde{W}_p is greater than G_0 is due to the fact that excitation of Δn modes in the language of geometrical optics is equivalent to scattering on Δn inhomogeneities. If an inhomogeneity with dimensions $L_z \sim L_{E \perp}$ is located close to the channel upper boundary, $\Delta n \sim 1$ and $\tilde{W}_p \sim G_0$.

4. Scattering of waves of the whispering gallery type by extended inhomogeneities of ionospheric plasma makes it possible (due to the aspect sensitivity of such scattering) to analyze the degree of excitation of the IVK in relation to mode number. We shall be interested in the relationship between excitation coefficient and plane wave angle of incidence on an inhomogeneity with incomplete coverage of wave channel volume by the inhomogeneity. Let r_1 be the distance from the upper edge of the inhomogeneity to the channel upper boundary, and L_z -- the longitudinal dimension of the inhomogeneity. The excitation coefficient differs from zero in the region of angles of incidence (φ_1, φ_2) at which stationary points determined by equation (25) (when a wave radiated by a ground transmitter strikes an inhomogeneity) fall within the region occupied by an inhomogeneity. Angles φ_1 and φ_2 are obtained with equation (25), which when

$|z_0 - z_n| \ll \pi$ has the form

$$r(r_{cr}) \approx M^2(z_0 - \varphi_n)^2, \quad (30)$$

where r_{CT} is the distance from point z_{CT} to the earth's center. Substituting in (30)

$r_{cr_1} = R_1 - r_1$ and $r_{cr_2} = R_1 - r_1 - L_z \cos \alpha_0$, we obtain

$$M |z_0 - \varphi_{1,2}| \approx \left[l_1 + \frac{k_0}{M} (r_{cr_{1,2}} - R_1) \right]^{1/2} = \xi_{1,2}, \quad (31)$$

FOR OFFICIAL USE ONLY

FOR OFFICIAL USE ONLY

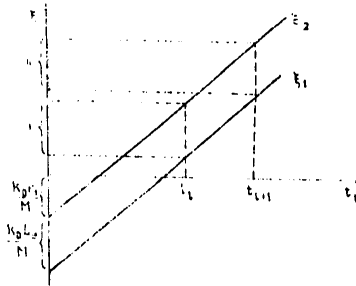


Figure 3.

Thus in order to excite particular types of waveguide modes (the presence of resolution by modes), it is necessary that regions of angles (φ_1, φ_2) satisfying different numbers l of waveguide modes, do not overlap. On the graph of relation $\xi_{1,2}(t_l)$ (Figure 3), plotted on the basis of (31), absence of overlap of regions I and II, corresponding with adjacent points t_l and t_{l+1} corresponds to solution by modes. With an increase in l , interval $\Delta t = t_{l+1} - t_l$ decreases, that is, there exists a limiting number beyond which a solution by modes is lost. As is evident from the graph, the greater the number of resolved modes, the smaller are L_z and r_1 . Inhomogeneity longitudinal dimension L_z , however, is bounded by a region important for integration,⁸ and further decrease in L_z corresponds to loss of aspect sensitivity. When

$$L_z = L_{z_{min}} \sim M l_1^{1/4} k_0$$

(inhomogeneity located close to the channel upper boundary), we have an equation which determines the number of resolved modes:

$$t_{l+1} - t_l \approx t_l^4. \quad (32)$$

An approximate estimate of solution of equation (32) (with utilization of asymptotic form $v(\xi_l)$), gives value $l^* \sim 5$. Thus positioning of the inhomogeneity with longitudinal dimension

$$L_z \sim M l_1^{1/4} k_0 \sim 0.5 \text{ cm}$$

close to the upper boundary of the channel corresponds to an optimal solution. The first five modes with angle of resolution $\Delta\phi = \phi_2 - \phi_1$, determined from (32), resolve well:

$$\Delta\varphi \sim \frac{1}{M} \sim 0^\circ.5.$$

FOR OFFICIAL USE ONLY

FOR OFFICIAL USE ONLY

In conclusion we shall note that the results obtained above also remain valid in a qualitative respect for a more realistic profile $\epsilon(r)$ of ionospheric plasma electron concentration in examination of propagation of waves of the whispering gallery type in the plane of a great circle.

FOOTNOTES

1. Here and henceforth we shall be examining monochromatic processes with time relationship $e^{i\omega t}$.

2. The method of disturbances within the framework of which expression (1) was obtained assumes a limit on transverse dimension of inhomogeneities $L_{\perp} = k_0 L_{\perp} \cos \alpha_0 \Delta \epsilon \ll 1$.

In actual fact inhomogeneities for which $k_0 L_{\perp} \cos \alpha_0 \approx 1$, contribute little to scattering which leads to waveguide washing or withdrawal of waveguide modes from an IVK. Therefore with condition $\Delta \epsilon \ll 1$ the above-indicated restriction to size of inhomogeneities can be considered satisfied.

3. Quantity $(1/3) (k_0^{-2} R_0)^{1/3} L_{E\perp}$ is a typical scale of transverse structure of the field of the waveguide under consideration.
4. As demonstrated in [1], waves of this type are the least attenuating in a supraterritorial wave channel.
5. For asymptotic form $J_{\nu_l}(k_0 R_1)$ we utilize here a more precise solution of dispersion equation $\nu_l \approx k_0 R_1 + \left(\frac{k_0 R_1}{2}\right)^{1/3} \left(t_l + \frac{1}{M}\right)$.
6. Condition (26) corresponds to a stationary point falling within the region of integration.
7. With this positioning a region significant for integration does not exceed the dimensions of the inhomogeneity.
8. In this region phase factor γ^z , standing under the integral (15), changes in value by order of magnitude π .

BIBLIOGRAPHY

1. Gurevich, A. V. GEOMAGNETIZM I AERONOMIYA, 11, 961 (1971).
2. Gurevich, A. V., and Tsedilina, Ye. Ye. GEOMAGNETIZM I AERONOMIYA, 13, 233 (1973).

FOR OFFICIAL USE ONLY

3. Borisov, N. D., and Gurevich, A. V. IZV. VUZOV -- RADIOFIZIKA, 19, No 9, 1275 (1976).
4. Yerukhimov, L. M.; Matyugin, S. N.; and Uryadov, V. P. IZV. VUZOV -- RADIOFIZIKA, 18, No 9, 1297 (1975).
5. Zaboronkova, T. M., and Kondrat'yev, I. G. IZV. VUZOV -- RADIOFIZIKA, 15, No 12, 1894 (1972).
6. Ludwig, D. J. MATH. PHYS., 11 (1970).
7. Yanke, E.; Emde, F.; and Lesh, F. "Spetsial'nyye funktsii" [Special Functions], Izd. Nauka, Moscow, 1977.
8. Getmantsev, G. G.; Yerukhimov, L. M.; et al. IZV. VUZOV -- RADIOFIZIKA, 19, No 12, 1909 (1976).
9. Zaboronkova, T. M., and Kondrat'yev, I. G. IZV. VUZOV -- RADIOFIZIKA, 20, No 12, 1895 (1977).
10. Gurevich, A. V.; Kim, V. Yu.; and Tsedilina, Ye. Ye. The Collected Volume "Sverkhdal'neye rasprostraneniye radiovoln i modeli ionosfery" [Extremely Long-Range Propagation of Radio Waves and Ionosphere Models], IZMIRAN, Moscow, 1977.

Scientific Research Institute of
Radio Physics
[8144/0533-3024]

Received 6 October 1978

COPYRIGHT: "Izvestiya vysshikh uchebnykh zavedeniy," "Radiofizika," 1979

3024
CSO: 8144/533

FOR OFFICIAL USE ONLY

Instruments, Measuring Devices and Testers; Methods of Measuring

UDC 621.391.264

ACOUSTO-OPTICAL FOURIER SPECIAL PROCESSOR

Kiev IZVESTIYA VUZOV SSR, RADIOELEKTRONIKA in Russian Vol 22 No 9, 1979
pp 68-69 manuscript received 7 Jul 78

[Article by V.P. Gubanov, T.N. Golovkina, A.Ya. Demidov, Yu.M. Polishchuk,
A.V. Pugovkin and N.Ye. Rodionov]

[Text] In this study is described a system for the spectroanalysis of continuous or pulsed radio signals, which operates in real time and includes an acousto-optical cell utilizing lithium niobate (used as a spectrum analyzer), a photodetector and a unit for linking with a computer which processes information on radio signal spectra.

Let us discuss the operating principle and key characteristics of an acousto-optical spectrum analyzer [1]. The structural diagram of such a spectrum analyzer is shown in fig 1. Radio signals directly from an antenna or through a wideband amplifier enter a piezoelectric transducer, 1, which converts the signal into elastic waves which are propagated in an acousto-optical medium, 2. The elastic wave, modulating the medium's refractive index in keeping with the dependence on the time, frequency and amplitude of the electromagnetic signal, creates a phase diffraction grating. The light beam from a laser source is broadened by means of a system of lenses, 3, to a diameter of a and strikes the ultrasonic cell at an angle of ψ relative to the normal to the wave vector of the elastic wave and is diffracted in the phase grating at an angle of 2ψ . The angle of diffraction is determined by the Bragg condition $\sin \psi = \lambda/2\Lambda = (\lambda/2V)f$, where λ is the wavelength of light in a vacuum, Λ is the wavelength of elastic oscillations, V is the phase velocity of an elastic wave and f is the frequency of the signal.

If a radio signal enters the inlet of the acousto-optical element, then each frequency component will be matched by a beam of light diffracted at angle 2ψ . The plane light wave striking the element will produce at the outlet a set of plane waves, and each frequency of the signal will be matched by its own plane light wave, and the spatial spectrum of the light at the element's outlet will reflect the frequency spectrum of the radio signal. Thus, the acousto-optical element is a kind of optical transparency functioning in real time.

FOR OFFICIAL USE ONLY

FOR OFFICIAL USE ONLY

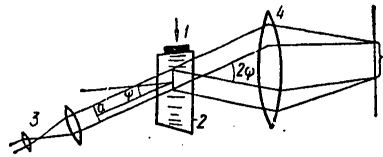


Figure 1.

Lens 4 performs a three-dimensional Fourier transform, forming in the focal plane a spatial spectrum of the light passing through the acousto-optical element. Each spectral component of the radio signal in the focal plane of lens 4 will be matched by a point of light. The distance between this point and the position of the non-diffracted ray equals

$$r = 2\lambda F/Vf, \quad (1)$$

where F is the focal length of the lens.

Thus, if a measurement is made of distance r in the lens's focal plane, it is possible to determine the frequency of the spectral component of the received signal. This operation can be performed by means of a position-sensitive photodetector, e.g., a vidicon or straight line of photodiodes.

Acousto-optical spectrum analyzers are characterized by sufficiently high speed of response and frequency resolution and make it possible to make a simultaneous analysis of the spectra of several radio signals arriving in the acousto-optical element's transmission band, as well as to determine the spectrum of a signal from a single arriving pulse. The speed of response of an acousto-optical spectrum analyzer is determined by a lag time of τ , during which the elastic wave fills from 10 to 90 percent of the light beam's aperture [1]:

$$\tau = 0.8a/V, \quad (2)$$

and its frequency resolution by the diffraction divergence of the optical beam:

$$\Delta f = V/a. \quad (3)$$

Below we will discuss the parameters of a spectrum analyzer developed for intermediate frequency radio signals. Its optical system is in no way

FOR OFFICIAL USE ONLY

FOR OFFICIAL USE ONLY

different from that shown above. As a light source is used an LG-44 laser. Collimator 3 and the diaphragm beyond it form an optical beam measuring $20 \times 2 \text{ mm}^2$. The acousto-optical element is made out of a crystal of lithium niobate. For the purpose of acousto-optical interaction is used the diffraction of an extraordinary light wave in slow elastic waves in the crystal's y section. The excitation of elastic waves is performed by an x section wafer of lithium niobate. The dimensions of the acoustic beam are 8 mm in the direction of light propagation and 2 mm in the perpendicular direction. The element makes possible an operating band for the spectrum analyzer, ΔF , of up to a few dozen MHz at frequencies of up to 4 GHz. The frequency resolution equals $\Delta f \approx 600 \text{ kHz}$ and is close to the theoretical. The effectiveness of diffraction at the central frequency with 1 W of input power equals 10 percent, which makes it possible to realize sufficiently high sensitivity to the input signal (approximately 1 mW).

As a photodetector is used a vidicon operating in the single-line scanning mode.

The characteristics and structure of the unit for linking the spectrum analyzer with a computer are determined from the following considerations. The rate of retrieval of information from the outlet of the spectrum analyzer is determined as follows:

$$c = 2 \frac{\Delta F}{\Delta T} \log h^l, \quad (4)$$

where T is the time for analysis of the acousto-optical element, h is the base of the code and l is the bit configuration of the code.

In place of the analysis time T included in equation (4), let us introduce parameter Δt , equal to the time spent for registering the spectrum, $\Delta t = (\Delta F / \Delta f v) \log h^l$, where v is the rate of entry of information into the computer.

For the purpose of matching the analysis time T and the registration time Δt , an intermediate information storage unit is required. This unit is the photodetector, which makes it possible to record information during time T and to read it out during Δt .

The most preferable area of application for this spectrum analyzer is the processing of short radio pulses or of random processes with brief steady-state intervals.

FOR OFFICIAL USE ONLY

FOR OFFICIAL USE ONLY

Bibliography

1. Dayson, R., Melon, B. and Mak-Magon, D. "Fizicheskaya akustika" [Physical Acoustics], edited by U. Mezon and R. Terston, Moscow, Mir, 1972, 7.

COPYRIGHT: IZVESTIYA VUZOV SSSR, RADIOELEKTRONIKA, 1979
[53-8831]

CSO: 1860
8831

FOR OFFICIAL USE ONLY

FOR OFFICIAL USE ONLY

Power Systems

UDC 620.9

PROBLEMS OF POWER ENGINEERING AT ITS PRESENT STAGE OF DEVELOPMENT

Minsk IZVESTIYA VYSSHIKH UCHEBNYKH ZAVEDENIY, ENERGETIKA in Russian No 7, 1979 pp 3-9

[Article by P. S. Neporozhniy, minister of power production and electrification of the USSR, Moscow Order of Lenin Institute of Power Engineering]

[Text] The decisions of the 25th CPSU Congress established the need for fundamental change in the fuel-power balance and in the direction of power engineering development in our country.

The Soviet Union possesses the largest fuel and power resources in the world. However, they are extremely unevenly distributed. The European sector consumes about 80 percent of the fuel and power resources, while their reserves comprise only 20 percent, and have a tendency to decrease in connection with intensive development. To the east of the Urals the relationship is reversed-- here, approximately 20 percent of the country's fuel and power resources are consumed, while 80 percent of the resources are located here.

Power production consumes almost half of the mineral forms of fuel in the country. The shortage of fuel in the European sector and the gradual shift to the east of chief fuel production bases are causing a significant increase in the volume of fuel transport. This leads to a sharp rise in the price of fuel and to a colossal strain on rail and pipe transportation, already operating at their potential limits.

The task has been set to sharply curtail the use of petroleum products as power station fuel supplies, owing to their short supply, to the growing volume of consumption in the chemical industry and to export deliveries.

The strain on the fuel-power balance and the need to curtail consumption of fuel oil have brought about development of the most important sector of the economy--electric power production--in the following basic directions in the foreseeable future (the next 10-12 years):

--the insuring of all growth of electric power production in the European portion of the country, owing to the accelerated construction of atomic power stations;

FOR OFFICIAL USE ONLY

FOR OFFICIAL USE ONLY

--the general development of hydroelectric power, the role of which is at a new stage of significant growth;

--the construction of powerful thermal electric power stations in the eastern regions, to be based upon cheap strip-mined coal and by-product gas from refining at Tyumen';

--the creation of extra-long, super-high voltage electric power lines for transit electronic transport of power from distant regions to centers of power consumption;

--further perfecting and completing the formation of a Unified USSR Power System.

Experience in developing Soviet power shows that electric energy production in our country doubles every 10 years. In the next 10-12 years the level of electric power production will considerably exceed 2 billion kWh [as published], including up to 600 billion kWh at atomic power stations and more than 300 billion kWh at hydroelectric stations. This will allow us to conserve up to 300 million tons of those conventional fuels that are in short supply, primarily fuel oil, and will ease considerably the country's fuel-power balance.

This will require that we bring the output of atomic power stations commissioned yearly up to 10-12 million kW, with an overall commissioning of 20-25 million kW of output power.

Atomic power stations (AES's). In connection with the need for fundamental change in the direction of power production development in the European section of the country, all growth of electric power production in this region will be accomplished owing to the commissioning of AES's, the output of which will reach 100 million kW in the next 10-12 years. At the end of the period being considered, more than 30 AES's will be put into operation.

The growth of AES's will take place due to the installation of shell-type and tubular-type thermal reactors with individual outputs of 1 and 1.5 million kW. Tubular reactors of 2.4 million kW capacity will be built.

The cost of electric power produced at the AES's with the powerful reactors will be within 0.45-0.60 kopecks per kilowatt-hour, while the cost amounts to 0.80 kopecks at thermal power stations.

At the present time AES's are being built with tubular reactors with which industry has become familiar. However, the major input of power (more than 50 million kW) will be produced owing to the installation of shell-type reactors, which are now being developed at the Novo-Voronezhskaya AES. A portion of such reactors will be used to create atomic central-heating plants (ATETs's).

FOR OFFICIAL USE ONLY

FOR OFFICIAL USE ONLY

At the Beloyarsk AES an essentially new type of pioneer fast-breeder reactor of 600 MW capacity is in operation. Based on the development of its design, commercial reactors of 0.8 and 1.6 million kW output will be built. The application of breeder reactors marks the advance of atomic power to a qualitatively new stage of development, since it produces more fuel than it consumes. This will practically eliminate the problem of nuclear fuel. However, for this it is necessary that power equipment builders, power-plant builders and workers from related sectors of industry carry out, in the period being considered, a great many research, design and planning projects for the development of the given type of reactor, and also develop the corresponding machine-construction base.

The AES Construction will be carried out in a continuous operation. Each year one 1-1.5 million kW reactor will be put into operation at each of the large-scale stations. This requires new organizational technology and the production of construction and installation projects, the creation of new construction and installation machinery and also the execution of large-scale organizational-technical measures.

The fulfillment of the planned program of AES construction is impossible without the further development of atomic machine construction and other sectors. Toward this end the USSR Ministry of Energy is carrying out the construction of the gigantic "Atommash" plant, the first production line at which will be commissioned at the end of the current year.

The corresponding sectors of industry must develop means of automation, as well as control and measurement instruments, etc., of great accuracy and reliability, intended specially for the AES's. These sectors must also master their production.

Hydroelectric stations (GES's). At its new stage of development, hydraulic energy is becoming particularly important. This has been brought about not only by the tension of the country's fuel-energy balance. Under operating conditions within the USSR's Unified Power System the hydroelectric stations carry out the following basic functions:

- covering a considerable portion of the peak periods on the daily load schedule;
- insuring the reliable functioning of the power system, thanks to the practically instantaneous engagement of the hydraulic units, accomplished automatically when emergency situations arise;
- bringing about automatic regulation of the power system's frequency and effective output in the normal operational mode in order to maintain the quality of electric power, etc.

FOR OFFICIAL USE ONLY

FOR OFFICIAL USE ONLY

The traditional role of the GES as a source of cheap electric energy for power-consumptive industry is retained only in the country's eastern region, where there is an abundance of hydroelectric energy, and also in distant regions with isolated power systems.

The specified GES output in the period of consideration will exceed 90 million kW, with the development of more than 300 billion kWh. The hydraulic resources of the European portion will be utilized practically in full (with the exception of the Caucasus region), while the peak of the daily load schedule will rise considerably. The normal operation of AES's in the European portion will be possible only in the presence of additional hydraulic capacity, which will be fed into hydro-accumulating electric power stations (GAES's).

While taking part in regulating a load schedule with doubled capacity (owing to peak coverage and an increase in the minimum load when electric power is used for charging) the GAES's should insure a uniform load on the atomic power stations, which are not adapted to operation in the shunt mode.

It is proposed that 14 GAES's with a fixed output of no less than 12 million kW be built. The further development of power production in the country's European sector is impossible without accelerated construction of GAES's.

In order to guarantee the planned program of increased capacity at GAES's, it is necessary to develop and introduce reversible hydro-units of increased capacity (more than 200,000 kW) and head (more than 400 m). The emphasis in hydroelectric station construction has been shifted into the eastern regions, where large-scale, high-pressure GES's with great reservoir capacity and inexpensive dams made of local materials are being built. An example is the Rogunskaya rock-fill dam and the Boguchanskaya dam, erected by hydromechanical means. At the same time, the dimensions of the agricultural resources trampled were held to a minimum.

A unique hydroelectric potential is possessed by the Angara-Yenisey basin, where continuous construction on more than 10 large-scale GES's is being developed, including the Turkhanskaya GES with an output of 10 million kW. Each of its power units is rated at 1 million kW. The total rated output of the GES's in the cascade comprises 60.5 million kW. Hydroelectric power is transmitted from here into the center of the country along super-capacity power lines.

In 1978 the Siberian power system was connected to the country's Unified Power System, and power from the Siberian GES's is already being transmitted to the European sector.

Thermal electric power stations (TES's) will retain the dominant position in rated output and production of electric power, though their share in the overall balance will decrease. In the European part of the country condensation TES's under construction will be finished presently; there will be no new

FOR OFFICIAL USE ONLY

FOR OFFICIAL USE ONLY

construction performed. A broad program has been planned for converting the operating thermal plants from fuel oil to coal and, if possible, to gas.

The introduction of new output capacities at thermal electric power stations will be carried out chiefly at the Ekibastuz, Kansk-Achinsk and Surgut fuel and power production complexes, where power units of great capacity will be employed.

Five electric power plants with 4 million kW output apiece and power units of 500,000 kW each will be built as part of the Ekibastuz fuel and power production complex. They will insure electric power for Kazakhstan and the Urals, and will convey electric power in transit to the country's central regions.

The construction of the power stations for the Kansk-Achinsk fuel and power production complex (KATEK) will be accomplished using 800,000 kW power units in 6.4 million kW electric power plants. At the end of the period under consideration it will be necessary to introduce here 10-12 million kW of new capacity. In prospect, the energy of the KATEK will be transmitted into the country's European sector.

In Tyumenskaya oblast, electric power stations will be constructed which will use natural gas and incidental gas from the petroleum refining process. Super-capacity power units of 1.2 million kW output will be employed.

In Central Asia, Yakutiya and the Far East, thermal electric power stations will be constructed to operate using local coal and also local sulfur dioxide.

About 4.5 million kW will be commissioned at special thermal electric power shunt stations (gas turbine installations and semi-peak steam-gas power units) with limited hours of utilization. In view of the fact that such power plants operate on types of fuel that are in short supply and are characterized by high specific consumption, their application is limited.

The planned program of thermal electric power plant construction requires that a great many research and design projects be conducted. The utilization of low-grade coal at high-capacity thermal electric power plants presents particular problems for the boilermakers. The boiler unit for the Ekibastuz stations has already been constructed. However, in view of a predicted further worsening in the quality of coal, an essentially new type of boiler unit must be developed. Experimental projects in this direction are now being carried out for the Kansk-Achinskaya thermal electric power plants, which will utilize the lowest grade of coal.

The main problem which must be solved during the construction of the KATEK is the development of no-waste methods of utilizing Kansk-Achinsk coal in power production.

FOR OFFICIAL USE ONLY

FOR OFFICIAL USE ONLY

District heating and power plants (TETs's). The Soviet Union occupies first place in the world in district heating and power plant output, which allows it to utilize fuel most economically in the combined production of electric energy and heat. The rated output of district heating and power plants and their production of thermal energy have doubled, exceeding 100 million kW and 1.2 trillion Gcal.

By the end of the 11th Five-Year Plan, atomic district heating and power plants with outputs reaching 13 million kW will be put into operation, and the construction of atomic heating stations will begin as well. In the near future the question must be decided: which of these two directions in heat extraction through atomic energy is the more efficient.

That portion of consumers covered by the centralized heat supply will reach 80 percent, as opposed to the existing 67 percent. Because of this, fuel savings on the order of 20 million tons of conventional fuel will be obtained.

Prospective sources for obtaining electric power. At the present time there is extensive work being carried out on the magnetohydrodynamic method of obtaining electric power. In combination with a thermal electric power plant, an MHD generator makes it possible to raise the electric power station's efficiency to 60 percent, as opposed to 40 percent at ordinary thermal electric power plants. By the end of the period under consideration it will be necessary to switch to the industrial production of electric power at MHD electric power stations.

Work is being continued on the utilization of geothermal, solar and wind energy. Besides the existing Pauzhetka geothermal electric power station on Kamchatka, a large-scale electric power station operating on underground heat is being erected in Dagestan. An experimental 200 kW solar electric power station is being built in the Crimea. Particular interest is offered by research in the area of controlled thermonuclear fusion: in the next decade one may expect the appearance of experimental thermonuclear power installations.

The development of electric power lines. In the next 10-12 years we foresee the commissioning of new types of electric power lines. These lines, with which we are still not familiar, carry 1150 kV of alternating current, 1500 and, in prospect, 2200 kV of direct current. They will be the world's longest and most powerful electric power lines.

The 1150 kV AC power line is intended for transmission of electric power from the electric power stations of the Ekibastuz, Surgut and Kansk-Achinsk fuel and power production complexes. We foresee the construction of a Siberia-Kazakhstan-Urals line 2400 km long and two Surgut-Urals lines, each 1300 km long. In order to master this sort of current during the present Five-Year Plan, a 270 km experimental-commercial power line from Itat to

FOR OFFICIAL USE ONLY

FOR OFFICIAL USE ONLY

Novokuznetsk must be put into operation, and the commercial manufacture of the necessary equipment and apparatus must be organized.

A 1150 kV DC power line 2400 km long from Ekibastuz to the Center will allow us to transmit up to 40 billion kWh annually of cheap electric power to the country's central regions. At present model experiments and preparatory work are being started.

On the basis of familiarization with power lines of the above-mentioned currents, we plan in the future to construct 2200 kV DC power lines to transmit 100 billion kWh of electric power annually from the Siberian stations to the European portion of the country.

In order to convey the output of atomic power plants, a 750 kV network is being created which will also be employed in consolidating the electric power systems of CEMA member nations with a USSR Unified Electric Power System.

Construction of 220,330 and 500 kV power lines will continue. In only 10-12 years about half a billion kilometers of electric power lines with voltages of 35 kV and higher will be built. In order to decrease network losses, it will be necessary to raise the reactive power compensation by a factor of two or three times in the near future.

At present the construction of 750 kV electric power lines has been sufficiently mastered. In order to turn the work toward the construction of 1150 kV AC and 1500 kV DC electric power lines it is necessary to conduct a number of scientific-research and design-construction projects for the development of new types of equipment. Minelektrotekhprom must develop production of the equipment for high-power electric lines in quantities that satisfy the country's power production requirements.

The USSR Unified Electric Power System (USSR EES) is the highest form of organization of the country's power production economy. The creation and functioning of the USSR EES is the strongest testimony to the advantages of the socialist order. All the measures described above for the development of power engineering in our country are, in the long run, intended to guarantee a reliable and uninterrupted electric power supply to consumers, accomplished by means of the USSR Unified Electric Power System.

Today the USSR EES unites a territory of 10 million square miles possessing a population of 220 million. Out of the country's 93 electric power systems, 77 are working in parallel. These stations comprise nine consolidated electric power systems (OES's) in which operate more than 700 electric power stations with a rated output of about 205 million kW and which develop 90 percent of the electric power produced in the USSR. The consolidated electric power system of Central Asia for the time being does not go into the USSR EES due to the distances involved. It will be connected in the 11th Five-Year Plan.

FOR OFFICIAL USE ONLY

FOR OFFICIAL USE ONLY

The link-up of the Far Eastern consolidated electric power system will take place during the 12th Five-Year Plan in connection with the electrification of the BAM.

By the end of 1978, the consolidated power system of the CEMA member nations had been engaged in parallel with the operation of the USSR EES.

The creation of the USSR EES has guaranteed us a number of important advantages. The power demanded from electric power stations has dropped significantly in comparison with those stations in operation within isolated electric power systems. This is due to output overcurrents covering the load-schedule maximums which arrive at various times and, consequently, to compensation of the daily schedule, as well as to emergency mutual assistance, repairs, etc. Because of this, the decrease in electric power station output at present amounts to 10-12 million kW, and will reach 30 million kW in 10-12 years.

The most modern equipment is getting maximum utilization and its performance is being improved. Thanks to this, great efficiency in the operation of Soviet power production is guaranteed to a considerable degree.

Conditions have been created for a reliable electric power supply to the economy, multiple reserves of electric power supplies for the most responsible consumers and the prevention of significant interruptions of the electric power supply, even when entire electric power stations unexpectedly drop out of service. Despite the fact that our reserves are considerably smaller than those of the USA, there were in the Soviet Union no massive system emergencies such as those which often occur in the United States.

There is, in the interests of the entire economy, an optimum utilization of water resources in the operation of hydroelectric stations. We have made it feasible to consume first those energy resources which at the given moment are most expedient in the economy. The USSR EES is efficiently co-operating with rail transportation and the oil and gasoline system, that is, the country's entire "circulatory system," under the unified management of high government organs.

Power engineering differs from other sectors of industry because of the continuous production processes and the distribution and consumption of electric power, as well as the strict correspondence between generation and consumption at every moment in time among a great many projects all over the country's territory. This peculiarity, as well as the rapidity with which emergency processes pass through the electric power system, has stipulated the high level of automation within the USSR Unified Electric Power System.

The management of power production is accomplished with the aid of an automated dispatch control system (ASDU USSR EES). The reliability of the power system, expressed in the guarantee of an uninterrupted power supply, is determined by

FOR OFFICIAL USE ONLY

FOR OFFICIAL USE ONLY

its stability and viability. A deciding role in this is played by the GES's and hydro-accumulating electric power stations, at which are located the operational power reserves. The mobilization of these reserves takes place in a matter of seconds. The hydroelectric power stations also provide 90 percent of the regulating capability of the automatic frequency and output adjustment system. The participation of the thermal electric power stations in covering the peak portions of the daily load for the Unified Electric Power System is associated with considerable over-consumption of fuel, and the role of hydraulic capacities is also extremely important here.

In order to guarantee the reliable functioning and completed formation of the USSR EES within the period under consideration, it is necessary to intensify the intersystem ties, unite the consolidated electric power systems of Central Asia and the Far East and complete the construction of the USSR EES automated dispatch control system, having first equipped it with the sufficient number of modern facilities for automation, protection, direction and communications.

This new stage in the development of power engineering in the Soviet Union is characterized by the stepped-up construction of atomic power plants in the country's European portion. Hydro-accumulating electric power stations must be put into operation to insure the normal functioning of these AES's. Thermal electric power production will be developed in the eastern regions through utilization of cheap low-grade coal, and large-scale hydroelectric power stations will be built on the Angara-Yenisey cascade as well. The formation of the USSR EES will be completed, and extra-long, super-capacity electric power lines will be built.

The tasks which have been set forth demand fundamental reconstruction of scientific-research, design-research and construction-installation projects and of power-production machinery construction on the part of the USSR Ministry of Energy and the cooperating sectors of industry.

The USSR Ministry of Power Engineering and Electrification and other ministries and departments must fully execute the program planned by the party in the area of power engineering--the basis for development of the country's productive forces. [67-9512]

COPYRIGHT: "Izvestiya vuzov SSSR - Energetika," 1979

9512
CSO: 1860

FOR OFFICIAL USE ONLY

FOR OFFICIAL USE ONLY

Publications

HANDBOOK ON ACOUSTICS

Moscow SPRAVOCHNIK PO AKUSTIKE (Handbook on Acoustics) in Russian 1979
signed to press 20 Feb 79 p 2, 311-312

[Annotation and table of contents from book by Viktor Kivovich Iofe,
Vadim Georgiyevich Korol'kov and Mikhail Andreyevich Sapozhkov, Izdatel'stvo
Svyaz', 31,500 copies, 312 pages]

[Text] The Handbook on Acoustics contains the basic data and materials on
acoustic oscillations, sound perception, acoustic signals and processing of
them, electroacoustical apparatus, sound amplification and sonication,
sound recording and reproduction, the acoustics of rooms, including radio
and television studios, acoustic measurements, sound-absorbing and sound-
insulating materials and structures. Formulas, graphs, tables and examples
of calculation are presented.

The handbook is intended for engineers and technicians working on the opera-
tion and design of means of communications and broadcasting and also radio
servicing. It will be useful to students of communications vuzes and
technical schools and to specialists of related occupations.

Contents	Page
Foreword	3
List of Notations	4
Introduction	5
Section 1. Acoustic Oscillations and Sound Waves	6
1.1. Definitions	6
1.2. Linear characteristics of the acoustic field	8
1.3. Energy characteristics of the acoustic field	9
1.4. Levels	10
1.5. The plane wave	12
1.6. The spherical wave	13
1.7. The cylindrical wave	15
1.8. Wave interference	16
1.9. Reflection of sound	16
1.10. Refraction of sound	18
1.11. Wave diffraction	19

FOR OFFICIAL USE ONLY

FOR OFFICIAL USE ONLY

1.12. Wave attenuation	20
1.13. Sound propagation in pipes	21
Section 2. The Main Properties of Hearing	23
2.1. Introduction	23
2.2. Perception by frequency	28
2.3. Perception by amplitude	39
2.4. Time characteristics of hearing	41
2.5. Perception of pulses	42
2.6. Nonlinear properties of hearing	43
2.7. The binural effect	44
Section 3. Primary Acoustic Signals and Their Sources	44
3.1. Introduction	44
3.2. The dynamic range and levels	49
3.3. The frequency range and spectra	55
3.4. The time characteristics of the acoustic signal	56
3.5. Spatial distribution of speech intensity about the head	60
3.6. The primary speech signal	62
3.7. The larynx as a source of acoustic oscillations	63
Section 4. Electromechanoacoustic Systems and Materials	63
4.1. Introduction	65
4.2. Electromechanical analogs	76
4.3. Electroacoustic analogs	76
4.4. Electromechanical transducers	79
4.5. Methods of compilation of analog circuits	
4.6. Materials used in electroacoustical apparatus and acoustic devices	81
Section 5. Microphones	84
5.1. Definitions, classification and main parameters	84
5.2. Sensitivity and resistance	87
5.3. Operating principles of a microphone	96
5.4. The directional properties of microphones	104
5.5. Technical requirements on microphones	110
5.6. Description of some types of microphones	137
5.7. Operation of microphones	143
Section 6. Loudspeakers and Telephones	143
6.1. Definitions, classification and main parameters	146
6.2. Main characteristics of telephones and loudspeakers	157
6.3. Requirements on loudspeakers and telephones	
6.4. Description of some types of telephones, loudspeakers and acoustic systems	162
6.5. Calculations and designs of acoustic formulations	179
6.6. Connection of loudspeakers to acoustic systems	187
Section 7. The Acoustics of Rooms	190
7.1. The characteristics of rooms	199
7.2. Absorbing materials and their designs	207
7.3. Sound-insulation of rooms	210
Section 8. Radio Broadcast and Television Studios	210
8.1. Types of studios	210
8.2. Optimum reverberation in a studio	210

FOR OFFICIAL USE ONLY

8.3.	Sound insulation of studios	212
8.4.	Electroacoustical equipment of studios and listening rooms	216
Section 9.	Sonication and Sound Amplification	221
9.1.	The main indices of sonication systems	221
9.2.	Characteristics of sonication of open spaces	223
9.3.	Concentrate sonication systems	223
9.4.	Zonal sonication systems	233
9.5.	Characteristics of room sonication	235
9.6.	Concentrated room sonication systems	235
9.7.	Distributed systems	236
9.8.	Sound amplification	241
9.9.	Sound amplification apparatus	246
Section 10.	Sound Recording and Reproduction	250
10.1.	Basic sound recording and reproduction systems	250
10.2.	Phonograph records	254
10.3.	Apparatus for phonograph reproduction	256
10.4.	Photographic phonograms	261
10.5.	Tape recorders	266
10.6.	Magnetic tapes	277
10.7.	Design of the sound recording control room	282
10.8.	Technology of magnetic sound recording	284
Section 11.	Transmission of Acoustic Signals	285
11.1.	Definitions	285
11.2.	Signal distortions	286
11.3.	Noise and interference in communications channels	290
11.4.	Permissible values of distortions of broadcast signals	291
11.5.	Intelligibility and distinctness of speech	292
Section 12.	Acoustic Measurements	296
12.1.	Measuring apparatus and equipment	296
12.2.	Methods of measuring the main characteristics of apparatus and rooms	299
Bibliography		309
[87-6521]		

COPYRIGHT: Izdatel'stvo "Svyaz'," 1979

6521

CSO: 1860

FOR OFFICIAL USE ONLY

HANDBOOK ON COMPONENTS OF MICROSTRIP EQUIPMENT

Moscow SPRAVOCHNIK PO ELEMENTAM POLOSKOVOY TEKHNIKI (Handbook on Components of Microstrip Equipment) in Russian 1979 signed to press 25 Apr 79 p 2, 335-336

[Annotation and table of contents from book by Ol'ga Ivanovna Mazepova, Valeriy Petrovich Meshchanov, Nina Ivanovna Prokhorova, Aleksandr L'vovich Fel'dshteyn, and Lev Rafaelovich Yavich, Izdatel'stvo Svyaz', 11,500 copies, 336 pages]

[Text] A method of engineering calculation and design of devices based on microstrip lines--directional transponders, bridges, dividers, power adders, bandpass filters, harmonic filters and so on--is outlined. Special attention is devoted to the effectiveness of the calculating methods, their uniqueness and economy.

Intended for engineering-technical personnel who design subassemblies and components on microstrip lines.

Contents	Page
Foreword	3
Chapter 1. Microstrip Lines	4
1.1. Basic definitions	4
1.2. A symmetrical microstrip line with internal rectangular conductor	8
1.3. A symmetrical microstrip line with round internal conductor	19
1.4. A microstrip line	20
Chapter 2. Coupled Microstrip Lines	32
2.1. Introduction	32
2.2. Systems of parameters	33
2.3. Conditions for matching and directionality of coupled lines	46
2.4. Symmetrical coupled microstrip lines with rectangular internal conductors	46
2.5. Symmetrical coupled microstrip lines with round internal conductors	52

FOR OFFICIAL USE ONLY

FOR OFFICIAL USE ONLY

2.6. Coupled microstrip lines	57
Chapter 3. Directional Couplers on Coupled Homogeneous Lines	71
3.1. General data	71
3.2. Definitions and notations	72
3.3. Frequency characteristics of crosstalk attenuation	73
3.4. Parameters which determine the geometric dimensions of the coupler	75
3.5. Results of synthesis	77
3.6. Stage connection of directional couplers on homogeneous coupled lines	94
3.7. Coupled lines with front coupling and shielding (diaphragm)	97
Chapter 4. Superwideband Directional First-Class Couplers	99
4.1. General data	99
4.2. Structure and parameters of symmetrical directional first-class couplers. Quadruple analogs	99
4.3. Methods of synthesizing symmetrical directional couplers	102
4.4. Comparison of symmetrical multistage directional couplers to smoothing couplers	103
4.5. Main results of synthesizing symmetrical directional couplers	112
4.6. Structure and parameters of asymmetrical directional couplers on coupled lines	115
4.7. Methods of synthesizing asymmetrical directional couplers on coupled multistage lines	117
4.8. Methods of synthesizing asymmetrical directional couplers on inhomogeneous coupled lines	118
4.9. Comparison of asymmetrical multistage directional couplers to smoothing couplers	120
4.10. Main results of synthesizing asymmetrical directional couplers	121
4.11. Stage connections of directional couplers	130
Chapter 5. Superwideband Directional Second- and Third-Class Couplers	132
5.1. General data	132
5.2. Diagram for synthesis of second-class directional couplers	133
5.3. Equal-wave characteristics of crosstalk attenuation	137
5.4. Maximum-plane characteristics of crosstalk attenuation	145
5.5. Enclosure of non-polar emissions	145
5.6. Multistage directional third class couplers	148
5.7. Excessive parameters of second- and third-class directional couplers	152
5.8. Problems of realizing second- and third-class directional couplers	157
5.9. Comparison of multistage first-, second- and third-class directional couplers	162

FOR OFFICIAL USE ONLY

FOR OFFICIAL USE ONLY

Chapter 6. Dividers and Adders	165
6.1. General data	165
6.2. Wave matrices of hexapoles and quadruples	165
6.3. Multistage annular power divider	168
6.4. Annular power divider on inhomogeneous lines	176
6.5. Binary power dividers	182
6.6. Dividers with optimum matching characteristics	184
6.7. Stage divider circuits on directional couplers	189
Chapter 7. Bandpass Microwave Filters	191
7.1. Definitions and notations	191
7.2. Formulation of input data in design of bandpass filters	194
7.3. Some types of Microwave bandpass filters	195
7.4. Substitution diagrams of volumetric Microwave resonators and bandpass filters	197
7.5. The Q-factor of resonators	198
7.6. The amplitude-frequency characteristics of real bandpass filters	203
7.7. Some additional calculating formulas	208
7.8. The bandpass and losses	211
7.9. The relationship between parameters of bandpass filters	215
7.10. Circuit methods of reducing thermal losses in bandpass filters	217
Chapter 8. Bandpass Filters on Coupled Lines	217
8.1. Filters on opposite bars	217
8.2. Tables. Sequence of calculating operations	219
8.3. Filters with parallel-coupled microstrip resonators	262
Chapter 9. Harmonic Filters	271
9.1. General data	271
9.2. Multistage filters	271
9.3. Limitations on realization	289
9.4. Method and examples of calculating multistage filters	292
9.5. Loop filters	297
9.6. Sectional construction of harmonic filters	300
9.7. Method and examples of calculating loop filters	320
Bibliography	325
[84-6521]	

COPYRIGHT: Izdatel'stvo "Svyaz", 1979

6521

CSO: 1860

FOR OFFICIAL USE ONLY

SIGNAL RECEPTION AND EVALUATION OF QUALITY

Moscow PRIYEM SIGNALOV S OTSENKOY IKH KACHESTVA (Signal Reception and Evaluation of Quality) in Russian 1979 signed to press 19 Apr 79 p 2, 236-237

[Annotation and table of contents from book by Vyacheslav Petrovich Shuvalov, Izdatel'stvo Svyaz', 4,600 copies, 240 pages]

[Text] Methods of evaluating the quality of signals are considered and recommendations are given on reception of them in discrete message transmission systems to increase fidelity. Along with mathematical analysis of the methods of evaluating signal quality, problems of technical realization of signal quality detectors are outlined and the results of experimental investigation which characterize the effectiveness of their reception are presented.

The book is intended for scientific workers engaged in problems of discrete message transmission.

Contents	Page
List of the Most Used Notations	3
Foreword	5
Introduction	6
Chapter 1. General Problems of Component Reception Theory with Evaluation of Signal Quality	12
1.1. Probability characteristics	12
1.2. Criteria of comparison and optimization of detectors with the indirect method of error detection	15
1.3. Synthesis of quality detectors of receivers with erasure in component signal reception	24
1.4. Control by the minimum and maximum	27
1.5. Losses with non-optimum evaluation of signal quality	30
1.6. The information content of parameters used to evaluate signal quality	36
1.7. Characteristics of evaluating signal quality by the probability of incorrect reception with more than two gradations of quality	42

FOR OFFICIAL USE ONLY

FOR OFFICIAL USE ONLY

Chapter 2. Phase Modulation	43
2.1. General data	43
2.2. Phase-modulated signal reception with evaluation of quality during narrowband fluctuating noise	45
2.3. Monitoring the quality of relative phase-modulated signals in correlation reception and with the effect of narrowband fluctuating noise	50
2.4. Phase-modulated signal reception with evaluation of quality in communications channels with pulsed noise	56
2.5. Quasi-optimum reception with evaluation of signal quality in the presence of pulsed noise	60
2.6. Monitoring the parameters of received phase-modulated signals in the presence of pulsed noise	62
2.7. The effect of intercharacter interference on the operating efficiency of a quality detector	69
2.8. Calculation of the probability characteristics in the presence of multiple noise in the channel	75
2.9. Determining the probability characteristics with regard to the effect of linear channel circuits with pulsed and fluctuating noise	80
Chapter 3. Frequency Modulation	83
3.1. General data	83
3.2. Optimum reception with evaluation of signal quality in the presence of narrowband fluctuating noise in the channel [3.20]	86
3.3. Monitoring individual parameters of received signals and their combination in a channel with narrowband fluctuating noise	91
3.4. Synthesis of a digital FM signal detector in the presence of fluctuating noise	98
Chapter 4. Binary Signal Distortions	101
4.1. Characteristics of the random process at the output of a binary device	101
4.2. Boundary distortions and breakup of binary signals	107
4.3. The mass of distortions and its relationship to boundary distortions and breakups	111
Chapter 5. Problems of Evaluation of Binary Signal Quality	120
5.1. Optimum recording and analysis of signal quality with independence of affecting readouts	120
5.2. Optimum algorithm for processing elementary components for the case when readouts form a simple Markov chain	125
5.3. The effectiveness of recording and monitoring of quality when selecting a step weighting function [5.2]	128
5.4. Other methods of analyzing binary signal quality	135
Chapter 6. Reception of Composite Signals with Evaluation of Quality	138
6.1. Evaluation of composite signal quality	138
6.2. Models of error flow and erasure flow	143
6.3. Calculating the probability characteristics with respect to code combination	148

FOR OFFICIAL USE ONLY

6.4. Comparing the efficiency of systems to code and indirect methods of error detection	152
6.5. Joint use of code and indirect methods of enhancing reliability	156
6.6. Algorithm for processing blocks with preliminary separation of code combinations of errors [6.19, 6.20]	161
Chapter 7. Some Problems of Evaluating Communications Channel Quality	167
7.1. Methods of analysis	167
7.2. Analyzing channel quality by frequency of measured values falling into the given range	173
7.3. Analyzing the quality of a channel with pulsed noise under conditions of parametric uncertainty	178
7.4. Analyzing channel quality by frequency of the appearance of breakups	184
Chapter 8. Use of Devices for Analyzing Signal Quality in Data Transmission Systems	187
8.1. General principles of constructing quality detectors	187
8.2. Description of some methods and devices for analyzing signal quality	192
8.3. Experimental investigation of systems with indirect method of error detection	201
Appendix 1. Mathematical Description of Some Types of Noise	209
Appendix 2. Derivation of Theorems on Evaluations	217
Appendix 3. Modelling of the Error Flow	218
Appendix 4. Analyzing the Effectiveness of the Integral Method of Recording When Selecting the Step Weighting Function	221
Appendix 5. Determining the Quality of Decoding Group Codes	223
Bibliography	225
Subject Index	233
[85-6521]	

COPYRIGHT: Izdatel'stvo "Svyaz'," 1979

6521

CSO: 1860

FOR OFFICIAL USE ONLY

UDC 533.9

ULTRALONG RANGE PROPAGATION OF SHORT RADIO WAVES

Moscow SVERKHDAL'NEYE RASPROSTRANENIYE KOROTKIKH RADIOVOLN in Russian 1979
signed to press 26 Mar 79 26 Mar 79 pp 2-4

[Annotation and Table of Contents from the book by Aleksandr Viktorovich Grirevich and Yelena Yevgon'yeva Tsedilina, Nauka Publishers, 3,650 copies, 248 pp]

[Text] The book is devoted to a systematic presentation of the theory of long range propagation of short radio waves. Particular attention is devoted to the study of the global laws governing radio wave propagation and the development of detailed procedures for the calculation of radio paths. The problems of the capture of radio waves, radiated from the earth, in an interlayer waveguide channel and their exiting the channel are discussed in detail, taking into account the influence of inhomogeneities, artificially created in the ionosphere when it is perturbed by high power radio waves.

Some 17 tables, 232 bibliographic citations and 97 figures.

Table of Contents

Foreword	5
Chapter 1 Introduction	7
1. Circumterrestrial signals	7
2. Specific features of long range radio wave propagation	15
Chapter 2 A Spherically Symmetrical Ionosphere	20
3. The wave equation in a spherically symmetrical ionosphere	20
4. The field of a radio wave in an ionospheric channel	25
5. The permeation of radio waves through barriers between channels. The capture coefficient	29
6. Beam trajectories. Pulse propagation	31

FOR OFFICIAL USE ONLY

FOR OFFICIAL USE ONLY

Chapter 3	A Horizontally Inhomogeneous Ionosphere	35
7.	Geometric optics	35
8.	The adiabatic approximation	39
9.	Lateral deviations of radio wave trajectories	47
10.	Radio wave capture in an ionospheric channel and radio wave exit from the channel	51
Chapter 4	Laws Governing Ultralong range propagation of radio Waves in the Ionosphere	59
11.	A study of the global characteristics of long range propagation	59
12.	Radio wave absorption	81
13.	The calculation of long range radio paths using the adiabatic invariant method	97
Chapter 5.	Radio Wave Scattering	111
14.	The influence of scattering on radiation capture in a channel	111
15.	The influence of multiplesscattering on the propagation of radio waves in a channel	124
Chapter 6	Nonlinear Phenomena	142
16.	Regular nonlinear refraction	142
17.	Nonlinear scattering of radio waves	151
Appendix 1.	The Distribution of a Field of Radio Waves in Coupled Waveguide Channels	
Appendix 2.	Analytical Models of Ionospheric Parameters	174
1.	A three-dimensional model of the distribution of the electron concentration of a quiet ionosphere	175
2.	A three-dimensional model of the distribution of the effective frequency of electron collisions	185
Appendix 3.	The Wave Theory of Short Radio Wave Propagation in a Horizontally Inhomogeneous Ionosphere, N.D. Borisov, A.V. Gurevich	195
1.	The wave equation in a weakly inhomogeneous ionosphere	196
2.	The quasi-spherical approximation	198
3.	The interaction of quasi-spherical modes in a real ionosphere	199
4.	Adiabatic modes of ionospheric waveguides	201
5.	Radio wave capture in a channel	211
Addenda		223
Bibliography		236
[101-8225]		
8225		
CSO: 1860		

COPYRIGHT: Nauka, Glavnaya redaktsiya fiziko-matematicheskoy literatury, 1979

FOR OFFICIAL USE ONLY

FOR OFFICIAL USE ONLY

THE DEVELOPMENT OF RESEARCH IN THERMOELECTRICITY IN THE USSR

Kiev RAZVITIYE ISSLEDOVANIY PO TERMoeLEKTRICHESTVU V SSSR in Russian 1978
signed to press 2 Oct 78 p 2, 136

[Annotation and Table of Contents from the book by Anatoliy Andreyovich
Buryak, Nauka Dumka Publishers, 136 pages, 1,000 copies]

[Text] Interest in new power sources has increased sharply in many nations of the world in connection with the intensifying energy crisis. This has resulted in the intensification of research in thermoelectricity. A large number of published works, in turn, is generating interest in the history of the problem. This monograph is an attempt to consider the development of this field of knowledge from the first experiments in thermoelectricity to its state of the art and the prospect is for the application of thermoelectric power sources in the USSR. In particular, the development of the physical and chemical, as well as the heat physics research in the major semiconductor materials, methods of designing the most important components of power units and the power units as a whole, the circuit designs for assemblies and devices, as well as the major steps in the development of thermoelectric generator construction are treated.

The book is intended for scientific, engineering and technical workers, engaged in problems of thermoelectric power engineering and the history of the science.

Some 33 illustrations, 9 tables; Bibliography: pp 126-134 (307 citations).

Table of Contents

Foreword	3
Chapter 1 A Brief Historical Outline of Thermoelectricity	
Major developmental trends in the electrical engineering	7
Research in the field of thermoelectricity	10

FOR OFFICIAL USE ONLY

FOR OFFICIAL USE ONLY

Chapter 2	A Study of the Properties of Thermoelectric Materials	
Thermoelectric materials		24
Low temperature materials		27
Intermediate temperature materials		32
High temperature materials		38
Metal alloys		42
Electrical conductivity		51
Thermal electromotive force and the thermoelectric figure of merit		58
Chapter 3	Methods of Calculating the Main Parameters of Thermoelectric Devices	
Thermocouples		62
Thermoelectric generators		69
Chapter 4	Thermoelectric Devices and Installations, and the Major Steps in their Design	
The structural design of thermoelectric generators		72
Basic configurations of thermoelectric power units		84
The first thermoelectric converters		89
Solar thermoelectric generators		93
Thermoelectric generators using organic fuel		100
Thermoelectric generators using nuclear heat sources		111
Bibliography		126
Major Conventional Symbols Used [99-8225]		135

COPYRIGHT: Izdatel'stvo "Naukova dumka," 1978

- END -